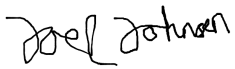






University of
Stavanger

Faculty of Science and Technology

BACHELOR'S THESIS

Study program/ Specialization: Mechanical Engineering and Material Science	Spring Semester 2021 Open access
Writer: JOEL JOHNSEN AMUND LØYNING HENNING GRANNE ANDRESEN	   Writer's Signature
Faculty Supervisor: Dimitrios G Pavlou External Supervisor: Ments Tore Møller	
Thesis title: Friction Modelling of Tension Wheel in Tether Management System	
Credits (ECTS): 20	
Key Words <ul style="list-style-type: none">● Tether Management System● Friction Modelling● Wire Rope Spooling● Rubber Materials	Pages: 99 +enclosure: 0 Stavanger May 14, 2021

Summary

This thesis investigates issues with IKM's current tether management system (TMS) design. This includes evaluating the current solutions, finding a suitable friction model through analysis and discussing material choices as well as drum rewinding algorithm alterations.

It has been established that the z-kink issues is most likely, as IKM engineers suspect, a product of squeezing the tether. The solution to this problem would be to limit the squeezing in a controlled manner, that inhibits z-kinks but allows for sufficient friction. Considering the analysis of different scenarios, it is proposed to use a U-shaped groove on the tension- and supportwheel that has a slightly smaller diameter than the tether itself, and move away from using the V-shaped groove on the wheels. This is likely allowing optimal service life and sufficient frictional properties. Material choices discussed in the thesis suggest that further testing is necessary to be able to find the best compound, but a tension wheel with a nitrile rubber basis with additives is most likely the best solution. Altering the rewinding algorithm to a non-lebusshell solution is discussed in detail, and it is concluded that the necessary cost of testing and research must be weighted against the cost of using the Lebus-shell.

As the thesis has a theoretical approach to the problems, it is more often than not necessary to do testing in order to optimize the solutions found. What types of tests that would need to be conducted is at part mentioned in the conclusion, and this could be done by IKM or future students.

Preface

This thesis is written to conclude our bachelors degree in mechanical engineering. The thesis is written by students at the Faculty of Science and Technology at the University of Stavanger.

The thesis has allowed us to put the theoretical knowledge and experience gained during our three years at the University of Stavanger to practical use. We are pleased to have been able to work with an external company, and talking to their engineers. We have learnt a lot during this semester, and we have found the work on the thesis both challenging and rewarding.

We would like to give a special thanks to our supervisor Dimitrios Pavlou for answering all of our questions, sharing his knowledge and providing crucial guidance. We also want to thank IKM Technology with a special thank you to our external supervisor Ments Tore Møller, for all our valuable meetings, both virtual and at IKM's ROV control room.

Stavanger, May 2021

Amund Løyning
Henning Granne Andresen
Joel Johnsen

Nomenclature

α	Fleet angle
α	The angle that describes the location in the U-groove
β	Half of groove-angle in V-belt transmission systems
Δ	Objects characteristic with respect to contact stress
δ	Depth of indentation
ϵ	Strain
γ	Desired thickness of material
μ	General coefficient of friction
μ_k	Kinetic friction coefficient
μ_s	Static coefficient of friction
ν	Poisson's ratio
σ	Stress
θ	Angle of contact between wire and pulley
A	Constant in contact stress equation
B	Constant in contact stress equation
E	Young's modulus
F	Force

H	Hardness of softer material in relation to two surfaces in contact
K	Constant related to wear of the material. Can have different units.
L	Sliding distance
L_{tether}	Circumference of tether
M	Mass
N	Normal force
$N(\alpha)$	Normal force distribution in a U-groove transmission system
N_{max}	Maximum normal force in a U-groove transmission system
Q	Volume wear
$Q\%$	Swelling ratio
R	All y-components of the normal force
R	Axial force in the tether
R'_1	Bending radius of object 1
R'_2	Bending radius of object 2
R_1	Radius of object 1
R_2	Radius of object 2
SIF	Stress intensification factor
SR	Slip ratio
T	Tension force in wire
V	Sliding speed
W	Force per unit length
W	Wear rate
b	Width of indentation
d	Distance in a pure rolling condition

e	Euler's number
f	Frictional force
f_k	Kinetic friction force
f_s	Static friction force
m	Mass
p	Nominal pressure at contact
r	Radius
s	Sliding distance
t	Time
v	Velocity
w	Actual angular velocity of rotational object
w	Wear
w_0	Angular velocity of a rotational object in a pure rolling condition

Contents

	Page
Summary	viii
Preface	viii
Nomenclature	viii
List of Figures	x
1 Introduction	1
1.1 Background	1
1.2 Scope of the work	2
2 Formulation of problem	3
2.1 What is a TMS	3
2.2 Introduction to how the M-TMS operates	4
2.3 Z-kinks	7
2.4 Rewinding without the use of Lebus Shell	8
2.5 Method for replacement of tension wheel	9
2.6 Alternative tension wheel designs	9
3 Theory	10
3.1 Friction	10
3.1.1 Coefficient of friction	10
3.1.2 Kinetic friction	11
3.1.3 Static friction	11
3.1.4 Rolling friction	13
3.1.5 Lubricated friction	15
3.2 Wear	16
3.2.1 Determining wear	16
3.2.2 Rolling contact fatigue	17
3.2.3 Wear indicators	17

3.3	Z-kinks	19
3.4	Pulley-system	20
3.5	Properties of rubber	24
3.5.1	Poisson's Ratio	24
3.5.2	Young's Modulus	24
3.5.3	Treloar's Equations - SIF	26
3.5.4	Frictional and wear properties of rubber	27
3.6	Drum	29
3.6.1	Lebus Shell	29
3.6.2	Tension during spooling	30
3.6.3	Fleet angle	30
3.6.4	Fleet angle compensators	31
3.7	Contact stress calculation	32
4	Assumptions	34
4.1	Capstan equation	34
4.1.1	U-shaped groove	34
4.2	Tether squeezing limit	35
4.3	Data from IKM	36
4.4	Material choice	36
5	Analysis and discussion	37
5.1	Z-kink issues	38
5.2	Evaluating the different solutions to the z-kink problem	41
5.2.1	V-shape with no squeeze	45
5.2.2	U-shape with no squeeze	46
5.2.3	Considerations of the no-squeeze design	47
5.2.4	Squeezing limit	47
5.3	Material suggestions	59
5.3.1	Wear	59
5.3.2	Friction	69
5.3.3	Material choice with respect to friction and wear	71
5.3.4	Method for when tension wheels should be replaced	72
5.4	Drum layout alterations	74
5.4.1	Smooth drum Lebus Shell layout	74
5.4.2	Smooth drum helical layout	75
5.4.3	Helical layout complications	76
6	Conclusions	83
6.1	Material choice	83
6.2	Choosing a friction model	83

6.3 Rewinding algorithm improvement	84
---	----

List of Figures

2.1	Design on today's TMS solution. Image provided by IKM.	4
2.2	Simplified layout of the M-TMS.	5
2.3	Z-kinks discovered by IKM upon inspection of tether. Image provided by IKM.	7
2.4	Simplified Lebus Shell drum layout	8
3.1	Two surfaces zoomed in.[15]	10
3.2	Forces drawn on a box in motion	11
3.3	Box placed in a hill	12
3.4	The relation between the friction coefficient and external force within Coloumb friction law.	13
3.5	A non-deformable object in a "pure rolling" situation.	14
3.6	A deformable object in a rolling situation.	14
3.7	Illustration of a full film fluid lubrication	15
3.8	Tread wear indicator on brakes.[20]	18
3.9	Tread wear indicators. [36]	18
3.10	Drawing of a belt drive	20
3.11	Cross-section of a V-belt	21
3.12	Force distribution in the U-groove.	22
3.13	Hysteresis descibed by a stress-strain curve.[31]	26
3.14	Layout of the Lebus Shell. [12]	29
3.15	Illustration of the fleet angle	30
3.16	Visualization of relevant radii for contact stress calculation	33
5.1	Free body diagram during rewinding.	42
5.2	Free body diagram of unwinding.	43
5.3	Visualization of tension wheel.	44
5.4	V-shaped tension wheel. This figure is not up to scale of the actual tension wheel	45
5.5	U-shaped tension wheel. This figure is not up to scale of the actual tension wheel	46

5.6	Cross section of Nexans RT-618 tether. Illustration provided by Nexans	48
5.7	Visualization of coefficients δ and b	50
5.8	Visualization of integration	52
5.9	Friction coefficient per indentation at nominal tether diameter	54
5.10	Overview of the different rubber materials that are compared in figure 5.11 [8].	60
5.11	This table shows comparisons of different rubber mixtures.[8] .	61
5.12	List of rubbers to comparison in figure below.[9]	62
5.13	Abilities of different rubber compounds rated from very good to not recommended.[9]	63
5.14	Different rubber compounds ability to abrasion resistance rated from poor to excellent.[26]	64
5.15	Wear rate with respect to PVC content. [16]	66
5.16	Swelling of NBR containing carbon black in 25°C [23].	67
5.17	Swelling of NBR containing carbon black in 70°C [23]	68
5.18	Comparison of different elastomers.[17]	69
5.19	Friction coefficient as a function of PVC content.[16]	70
5.20	Idea for wear indicators on the tension wheel	73
5.21	Simplified helical smooth drum layout.	75
5.22	Smooth drum layout. [38]	76
5.23	Simplified force scenario into a wedge in a helical layout	77
5.24	Simplified force scenario out of a wedge in a helical layout . . .	79
5.25	Smooth versus Lebus layout	81

Chapter 1

Introduction

1.1 Background

Ever since the deep-water industries, such as the oil and gas industry, started to grow and become giant industries, the need for underwater vehicles have been present. These underwater vehicles are used in various subsea-operations for various tasks. The underwater vehicles are divided into two categories, autonomous underwater vehicles (AUVs), and remotely operated vehicles (ROVs), with the difference being that the ROV is a tethered vehicle while the AUV is non-tethered. In the ROVs the umbilical cable can be directly connected to the vehicle from the ship or the platform. If the ROV is to operate in deeper-water or under tougher conditions, a tether management system (abbreviation TMS) is often used. This system is connected to the ship or platform via an umbilical cable, and connects to the vehicle via a neutrally buoyant tether, which helps reduce drag on the vehicle during operation. The TMS contains a drum that the tether is wrapped around, and the TMS then feeds tether to the vehicle depending on the depth of operation.

This thesis is written in collaboration with IKM. IKM have been designing, constructing and operating a variety of different tether management systems over the years. One of the more recent design, and the design that will be looked into in this thesis is the TMS made for Merlin, an electric work class ROV.

1.2 Scope of the work

The main focus of this thesis is to study the Merlin TMS, or M-TMS, developed by IKM and develop a better knowledge of how the unit works. The goal is then to use that knowledge to try to solve the problems that IKM are experiencing with the M-TMS. The problems are mainly related to three of the main components in the TMS;

- The tether
- The drum
- The tension wheel

In addition to perform closer study of the unit, the following problems are to be addressed in the thesis:

- Finding a model to calculate the squeezing limit before z-kinks gets formed in the tether.
- Find alternative designs that could improve friction between the tension wheel and the tether while reducing the squeezing effect.
- Come up with methods to optimize lifespan of the tether.
- Come up with a method to determine when its due for the tension wheel to be replaced, as well as study different rubber mixtures suitable to use for the tension wheel.
- Improve the current algorithm for rewinding of the tether, without the use of Lebus Shell.

Chapter 2

Formulation of problem

2.1 What is a TMS

A TMS, abbreviation for a Tether Management System, is a unit used in the deployment of a ROV. As introduced earlier, the TMS allows for the ROV to operate with less drag than with a direct deployment with a umbilical connected to the ROV. The TMS generally comes in two different forms; cage-TMS and tophat-TMS. The M-TMS that will be looked into in this thesis is a tophat-TMS, which is a type of TMS which sits on top of the ROV when deployed into the sea.

2.2 Introduction to how the M-TMS operates

The M-TMS is as described based around a drum carrying tether, and multiple wheels that ensure the tether follows the desired trajectory. A side view of the M-TMS is shown in Figure 2.1. There are two electrical motors installed on the M-TMS that provides the torque necessary to wind the tether, and one that are attached to the spool. One of the motors is connected to the drum itself, and one of the motors are connected to the tension wheel. As the tether travels in or out of the drum, it is in a state of tension inside the TMS. This is important as the tension allows for proper winding both on and off the drum. If the tether where to be slack at some stage during rewinding, this could lead to improper tether placement on the drum which could lead to complications for the operation due to damage on tether. To obtain this tension, the tension wheel and the adjacent support wheel in Figure 2.2 are equipped with V-shaped grooves to squeeze the tether to increase the normal force, and consequently leading to the grip needed for tension in the tether. The spool goes back and forth between the flanges of the drum, and provides proper placement on the drum by providing the proper fleet angle for the winding. Just above the support wheel in Figure 2.2 there are two other perpendicularly mounted support wheels. These wheels help the tether get firmly placed on the support wheel when the spool moves side to side.

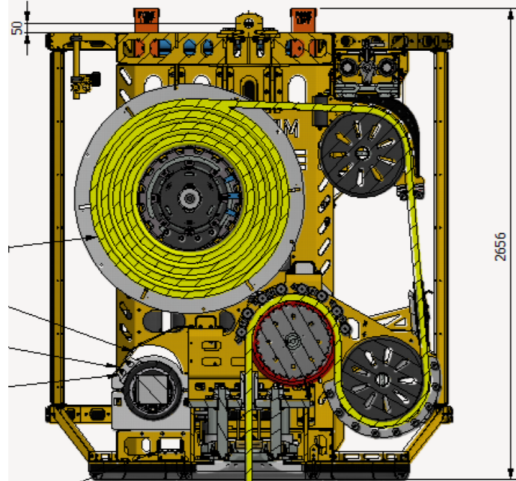


Figure 2.1: Design on today's TMS solution. Image provided by IKM.

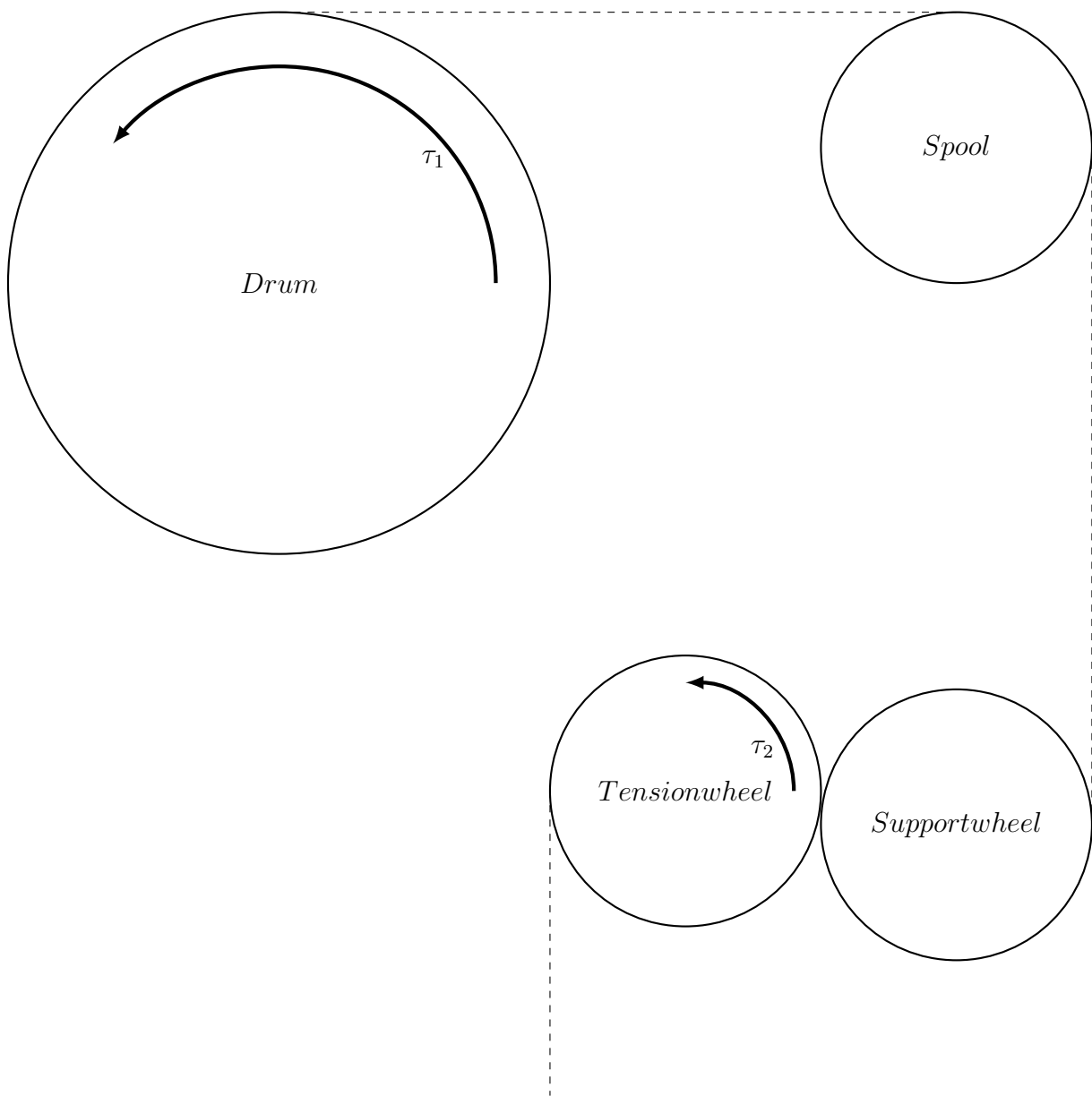


Figure 2.2: Simplified layout of the M-TMS.

As mentioned earlier, the tether needs to be in constant tension when being reapplied to the drum. In the rewinding process, the motor on the drum provides torque and this will try to initiate movement in the tether, as visualized in Figure 2.2. To be able to move the tether, the torque must overcome the friction in the system, and also the countering torque that the tension wheel is providing. Tension in the tether will in this situation be given by the two opposing torques minus the friction in the system. The tension in the tether ensures that it rewinds in a controlled fashion, and is placed properly on drum.

During the unwinding-process it is the tension wheel that does the heavy work by bringing the tether out. In the unwinding-scenario the torque on the tension wheel visualized in Figure 2.2 is in the same direction, while the torque on the drum is flipped. This is done so that the drum assists the tension wheel slightly so that the tether does not slip on the tension wheel. The torque provided by the drum in this scenario does not overcome the rolling resistance of the drum, and thus still allows for sufficient tether tension.

Data collected at IKM's onshore control room shows the loads working on the tether during the rewinding process. The rewind can be done at different speeds, which will determine how large the force acting from the drum and tension wheel will be. Regular operation loads was observed to be 200 to 350 kilograms of force from the drum, and between 100 to 200 kilograms of force from the tension wheel. The tension wheel pull on the tether with its given load at a set speed. The drum then pulls on the tether between itself and the tension wheel, to keep tension in the tether while being winded on the spool. IKM has observed that less than 200 kilograms of tension in the tether as it is being rewound, could lead to problems arranging the tether neatly on the drum.

2.3 Z-kinks

One of the main design flaws in today's M-TMS solution is the fact that IKM experiences z-kinks on the innermost conductors in the tether. In short these z-kinks can cause major damage in the conductors potentially leading to power loss and ultimately to the tether needing to be replaced. There are a wide range of different mechanical loads that can lead to z-kinks, but it is postulated by IKM that the problem of z-kinks is originating from when the tether goes between the tension wheel and the support wheel. The grooves of the two wheels are made in such a way that the tether gets squeezed,

and because of this the innermost cables are damaged. The assumption that the squeeze is the main cause of z-kinks comes from the fact that it is only the innermost cables of the tether that has experienced z-kinks. If either too high axial-loads or too small bending diameters were the main reason behind the z-kinks, the z-kinks distribution in the tether cross-section would likely be different than the z-kinks distribution experienced on today's M-TMS solution. This is due to the fact that the axial force is equal over the cross section, and the bending diameter is at its most extreme in the outermost layers of tether. Data backing up these claims are provided and analysed later on in the thesis. An image of a z-kink found in the tether is shown in figure 2.3.



Figure 2.3: Z-kinks discovered by IKM upon inspection of tether. Image provided by IKM.

2.4 Rewinding without the use of Lebus Shell

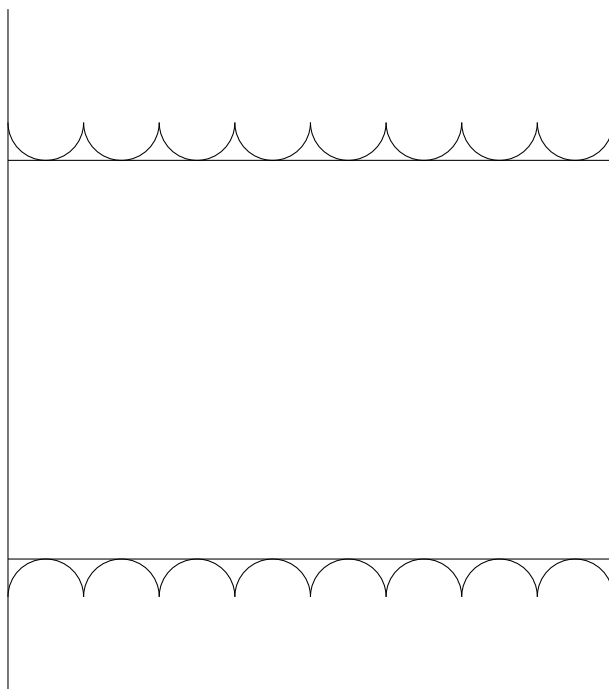


Figure 2.4: Simplified Lebus Shell drum layout

The M-TMS is in the current design equipped with a unit called the Lebus Shell. The Lebus Shell is wrapped around the drum, visualized in Figure 2.4 and creates a groove for the first layer of tether. The pattern is parallel to the flange, with two crossover sections per revolution. The Lebus Shell makes the winding of the tether go effortlessly and is in and of itself a very useful unit that removes much of the inconvenience with the initial winding of the tether around the drum. While the Lebus Shell is a useful unit, it also poses some problems, namely economic ones. First of all the unit is very expensive, which makes it less desirable to ac-

quire. In addition to it being expensive, one Lebus Shell can only work with one configuration of tether diameter, and limits the freedom of other alterations. If the operators, IKM, were to see it fit to change the tether to a new diameter or need to alter drum size, the Lebus Shell-unit poses a problem. The problem would be that the change in configuration would lead to the need of a purchase of a brand new Lebus Shell, which then also could only be used on that one configuration. Although being practical for a given configuration, the use of Lebus Shell increase cost for the firm and is not very versatile. IKM is therefore looking for a M-TMS configuration which is not dependent upon the Lebus Shell to operate smoothly in the winding-process. Due to the complexity of this alteration, a winding algorithm without the use of Lebus shell will not be provided, as it is simply not feasible to provide this without real life analysis of the setup. A part of this thesis will therefore be to compare the Lebus drum with a smooth drum layout, and discuss the advantages and disadvantages in regards to both layouts.

2.5 Method for replacement of tension wheel

The M-TMS is responsible for both the unwinding and rewinding of the tether, and both of these processes cause wear on the tension wheel as there are frictional forces constantly working on the surface and therefore deteriorating it. This will cause abrasion, which again may lead to the tether slipping on the tension wheel due to reduction in coefficient of static friction and reduced normal force. Ultimately this may lead to the tension wheel needing replacement, as the frictional forces at work can cause extensive wear on the wheel. There will therefore be devised a method to determine when the tension wheel should be replaced.

2.6 Alternative tension wheel designs

There are several ideas of alternative designs from IKM that will be looked at. As mentioned earlier, the V-shaped tension wheel in combination with squeezing is presumed to be the cause of z-kinks in the tether, and therefore a U-shaped design for the tension wheel will be investigated. The areas of concern with the U-shaped model are the friction and wear properties of the new design. To analyse this, it will be calculated what minimum friction coefficient is needed to operate the TMS safely using no squeeze at all for both the V- and U- grooved wheels. These solutions will be compared to a U- grooved tension wheel in combination with the squeezing effect. This includes calculating the amount of squeezing allowed, and what friction coefficients would be necessary to operate the TMS in this case.

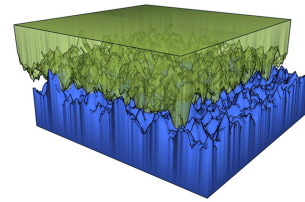
Different material types that may be used in the tension wheel will be discussed. The tribological properties will be the main focus including abrasion resistance, compact set, creep, adhesion, tear resistance and solvent resistance against water and oils. Optimizing the rubber compound could enhance life-span and maximize the effect of the desired rubber properties.

Chapter 3

Theory

3.1 Friction

Friction is a force between the surfaces of two objects which prevents the objects moving relative to each other.[14] Friction occurs because the surfaces are uneven. These uneven surfaces in contact grind each other. Different materials have different smoothness that will cause more or less friction.



The friction force is dependent on the friction coefficient and the normal force of the object. The friction coefficient is a representation of how the two surfaces resist motion in relation to each other. [13] The normal force is a measure of how much the object is pushing down on the surface at which it rests or slides. There are two different main types of friction, static and kinetic friction.

Figure 3.1: Two surfaces zoomed in.[15]

3.1.1 Coefficient of friction

The coefficient of friction is a unitless number that describes the relation between two perpendicular forces, the friction force and the normal force. [5]

$$\mu = \frac{f}{N} \tag{3.1}$$

where μ is the friction coefficient, f is the friction force and N is the normal force. The friction coefficient describes how the two surfaces slide against

one another under different loads. The coefficient of friction in a static relationship between two surfaces is usually higher than the coefficient of friction in a kinetic one with the same two surfaces. This means that

$$\mu_s > \mu_k \quad (3.2)$$

3.1.2 Kinetic friction

Kinetic friction occurs when there are two surfaces in motion relative to each other. When an object is in motion the friction force will point in the opposite direction of what direction the object is moving. This prevents the object from moving at a constant velocity along a horizontal surface. Rearranging equation 3.1 gives an expression of the kinetic friction.

$$f_k = \mu_k \cdot N \quad (3.3)$$

Here, μ_k is the coefficient of kinetic friction, N is the normal force, and f_k is the kinetic friction force. This equation is called the Coulumb friction law.[39]

The coefficient of kinetic friction will generally decrease with increasing velocity,[14] therefore velocity will have a vital role when determining the friction coefficient between two surfaces in relative motion.

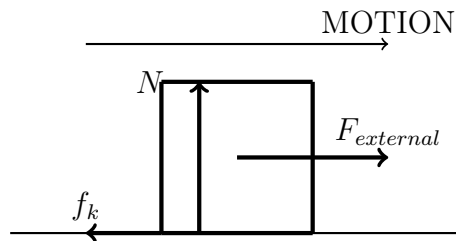


Figure 3.2: Forces drawn on a box in motion

3.1.3 Static friction

A force of static friction can be observed when another force is being applied to an object but the object does not move. The reason the object is not moving is because of static friction. For example, a parked car in a hill would be subjected to static friction. The static friction equation is similar to the kinetic friction equation and is described by

$$f_s \leq \mu_s \cdot N \quad (3.4)$$

Here, f_s is static friction force, μ_s is the coefficient of static friction and N is the normal force. When the surfaces are about to slip against each other, the equality is valid. This is known as impending motion. The inequality is valid when the surface is not about to slip.[30]

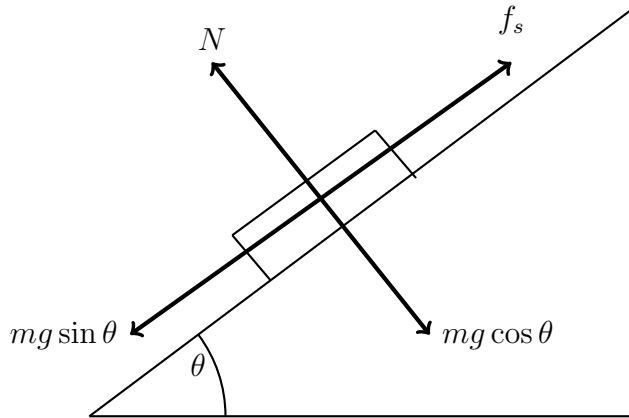


Figure 3.3: Box placed in a hill

Looking at Figure 3.3, imagine that θ started at 0° , and slightly increase θ . The static friction force, f , will increase as $mg \sin \theta$ increases. That means $f = mg \sin \theta$ at all times until θ is so big that f reaches maximum potential. When $mg \sin \theta > f_{max}$ the external force on the box will get so big that the box will start moving downhill. A similar situation is plotted in a graph in figure 3.4

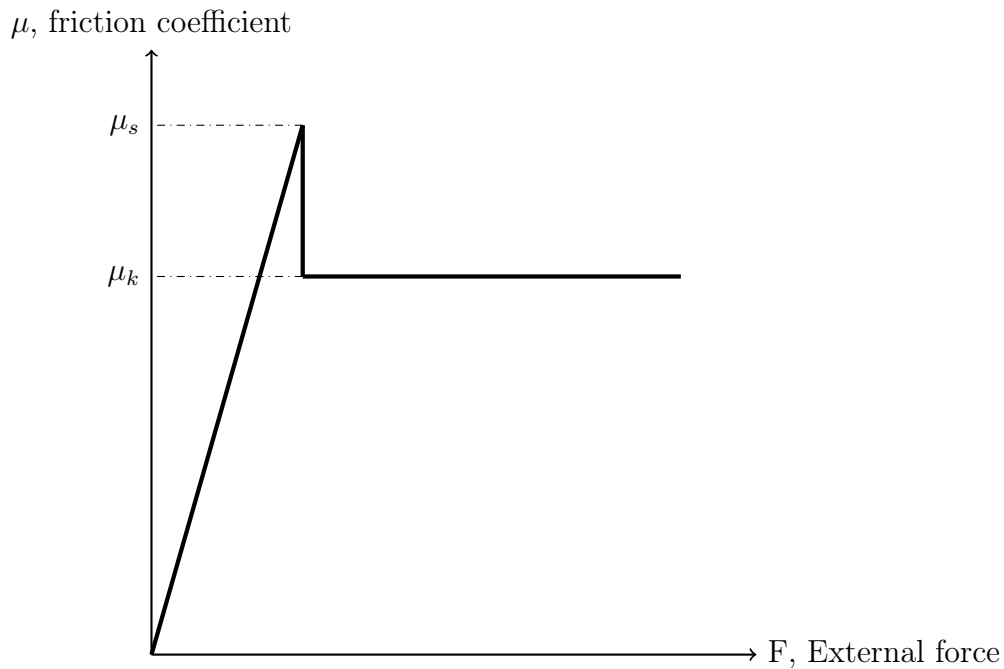


Figure 3.4: The relation between the friction coefficient and external force within Coloumb friction law.

3.1.4 Rolling friction

An example of where rolling friction can be observed is the car tires. When a circular object rolls on a surface, the friction in this system is called rolling friction. When a round rigid object is rolling on a surface with constant velocity, and the contact area is a line, it is called "pure rolling". In pure rolling there is no slip of the two surfaces and it follows that $\mu_k = 0$ and $d = 2\pi r$, where d is distance traveled, and r is the radius of the rolling object. When "pure rolling" occurs, the frictional force does not do any work, and therefore there is no energy loss. For "pure rolling" to be valid, the solid must be a rigid body. That means it cannot change shape by inducing an external force on it.[18] Figure 3.5 describes the contact between the rolling object and the surface at which it rolls. The contact area can be visualized as a line shown as the red line in the figure.

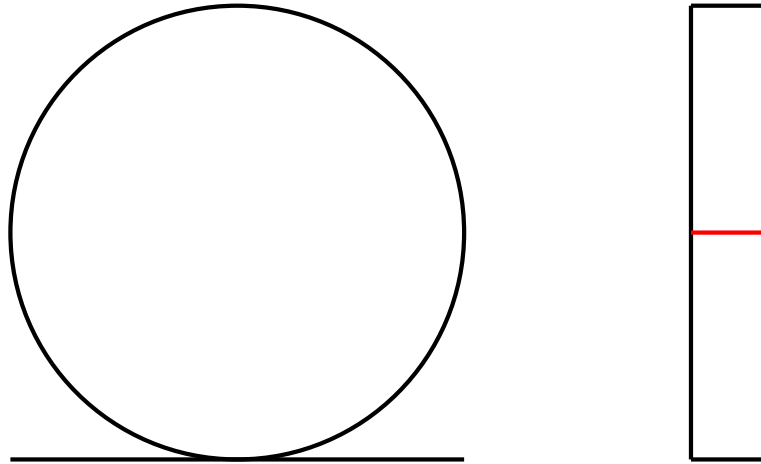


Figure 3.5: A non-deformable object in a "pure rolling" situation.

For deformable objects "pure rolling" does not occur, and instead of a line of contact, it is an area of contact. In this situation there will be small areas where sliding occur. The rolling object will be experience energy loss mostly due to deformation of the materials.[18] Figure 3.6 show the contact area as the area of the red square drawn.

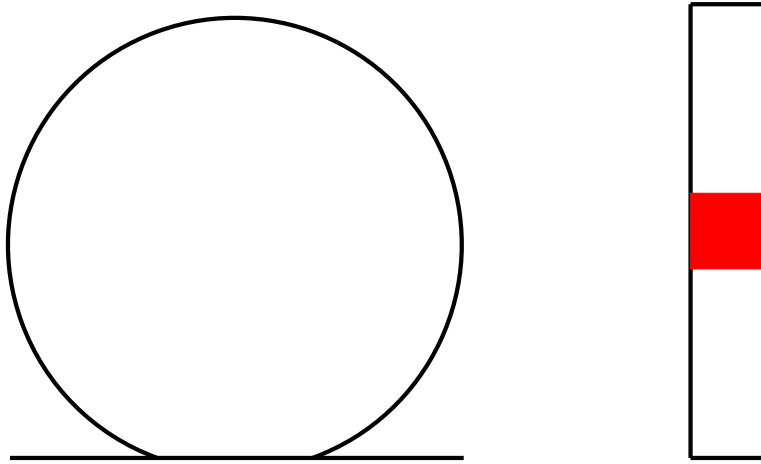


Figure 3.6: A deformable object in a rolling situation.

When deflection in the material happens, the slip-ratio will be important. The slip ratio describes the angular velocity of the rolling object against the actual velocity, and can be defined as: [4]

$$SR = \frac{w - w_0}{w_0} = \frac{w}{w_0} - 1 \quad (3.5)$$

where w is the angular velocity of the wheel, and w_0 is the angular velocity if the wheel were in a "pure rolling" condition. [4] Knowing this, the equation can be written as

$$SR = \frac{wr}{v} - 1 \quad (3.6)$$

where w is the angular velocity of the object, r is the radius of the object and v is the velocity of the object.

3.1.5 Lubricated friction

Lubricated friction prevents direct contact between the two surfaces, and will therefore be fluid friction, and not regular dry friction. This affects the normal force as well as the tangential forces. Lubricated friction decreases frictional forces and the wear of the surfaces involved. [25] Lubricated friction, also called lubrication is usually used to control friction and wear by introducing a film between the two surfaces such that the two surfaces are not in direct contact with each other. [7]

The substances used for lubrication vary greatly, among them can be both fluids and solids. Lubrication can be split up in three types; boundary, mixed and full film lubrication. A film would be a stream of fluid or solid between the two surfaces. The difference between these three, mainly involves how much interaction the two surfaces have with each other. From boundary lubrication, which offers more contact between the two surfaces, but still has lubrication in between the surfaces, to full film lubrication, which occurs when the two surfaces are a full film of fluid apart. Mixed lubrication would be a middle ground of boundary and full film lubrication. [7]

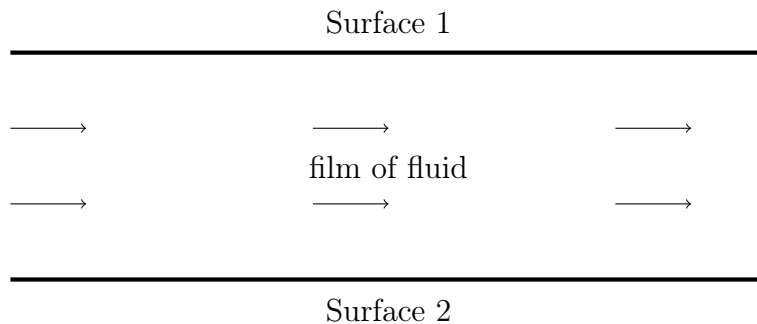


Figure 3.7: Illustration of a full film fluid lubrication

Full film lubrication can again be split up in to two forms, hydrodynamic and elastohydrodynamic. Hydrodynamic lubrication takes place when the

two surfaces are in motion relative to each other. Elastohydrodynamic exist when there are rolling contact between the two surfaces[7], for example a car's wheels on a wet road.

3.2 Wear

Wear is usually divided in the groups of mechanical wear and the situations which contains aspects of chemistry, such as corrosion. Mechanical wear can itself be divided into several branches such as abrasion wear, erosive wear, adhesion and surface fatigue. Abrasive wear takes a difference in two- or three-body abrasion. Two-body abrasion is when the softer surface's material is lost due to bumps or roughness of the harder surface. Three-body abrasion occurs when particles, that can come from the outside environment, displace or skim one or both of the surfaces involved. [40]. Erosive wear happens when the wear is a result of relative motion of fluid which holds solid particles in them, like sand or similar[11]. Looking at the definitions, it can be hard to determine the difference between erosive wear and three-body abrasive wear, and velocity of the particles are important to distinct these two. [40] Surface fatigue appear as there are cyclic loading that can be caused by rolling contact, sliding contact or a combination between the two bodies. [27] How much a material deteriorates, in other words the wear, is dependent on many factors. These factors are for instance normal load, sliding speed relative to the surfaces, geometry, temperature and environment the surfaces appears in as well as chemical, thermal and mechanical properties of the two bodies concerned. [40]

3.2.1 Determining wear

Determining the wear has been experimented with for a long time. One way to resolve the wear is known as Archard or the Rabinowicz equation. The equation comes in many different forms, one of them is given by

$$\frac{w}{t} = K \cdot \frac{pV}{H} \quad (3.7)$$

where K is a constant, t is time, p is the nominal pressure at contact, w is the wear dimension, V is the sliding speed and H is the hardness of the softer surface involved.[40] Another way the equation is submitted is

$$Q = K \cdot \frac{Fs}{H} \quad (3.8)$$

where Q represents the volume wear, K is the wear coefficient, F is the normal force acting on the surface, s is the distance of sliding and H is the softer surface's hardness.[2] Although there are several different ways to formulate the Archard equation, and thus the units change depending on which version, the wear coefficient K describes the materials ability to resist wear,[24] that is often affected by the environment and situation.[2]

3.2.2 Rolling contact fatigue

Rolling contact fatigue, also known as RCF, is a type of wear of materials caused by rolling contact between two surfaces. The wear comes from the stress that is formed from the friction forces, and this can cycle as the contact surface is changing. Cyclical scenarios may cause cracks of the material that spreads from this weaker point. Another consequence can be deterioration of material, that may account for a more polished surface of the material. [6] Because of rolling contact, and especially for non-deformable materials, the "slip ratio" must be taken into account. Since static friction and kinetic friction are two very different phenomena, this ratio has an effect on the wear of the material used.

3.2.3 Wear indicators

Wear indicators are used in several different mechanical constructions and parts such as tires, called tread wear indicators, and brakes, called brake wear indicators. Wear indicators gives the user an idea for when the particular part has been worn down extensively to the point where it is non-usable anymore. When the brake pad in figure 3.8 is worn down the brake wear indicator will touch the brake disc and make a squeaky noise.

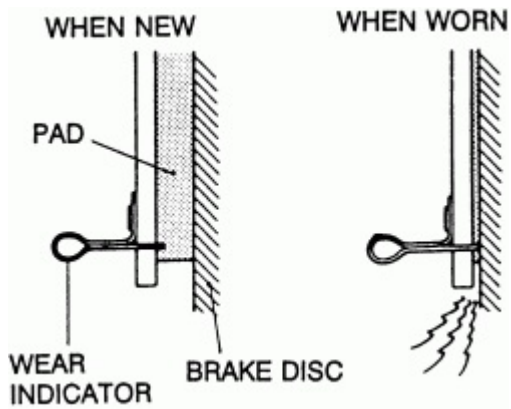


Figure 3.8: Tread wear indicator on brakes.[20]



Figure 3.9: Tread wear indicators. [36]

3.3 Z-kinks

A z-kink appears where a cable or wire has been subjected to a force that exceeds the conductors yield strength. Oftentimes this means that the copper conductor inside the cable will elongate plastically. When the force acting on the cable is reduced, and the cable retracts, the conductor inside the cable will stay elongated. The elongated conductor is too long to follow its original trajectory, which cause it to find a place it will be able to fit. This elongation can migrate along the cable to find a suiting place for it to stay, and thus creating the z-kink at this point along the cable.

The force acting on the cable creating a z-kink can be one instant heavy tensile load, cyclic tensile load, twisting, bending or compression loads. The most intuitive way of picturing a z-kinks formation will be when a cable is subjected to axial load. The load is evenly distributed along the cross sectional area, and when the conductor yield strength is achieved, the conductors elongate. Bending a cable over a small radius may also cause kinks, as the outermost and innermost conductors are subjected to tension and compression forces. The greater the bending radius the more homogeneous the force distribution will be on the cables cross-sectional area and the lesser danger of bending creating z-kinks.

A tether used for ROV operations will be affected by different forms of tension during operation. Therefore, one must look at the combined forces of axial tension, bending, compression and any other forces present in order to get a complete picture of how the cable will behave and respond.

Z-kinks may lead to severe damage of the conductor, which may render the tether unusable. In the case of the ROV this could lead to a loss of communication with the ROV unit, loss of power or complete blackout. The z-kink issue is therefore of highest priority to solve.

3.4 Pulley-system

Pulley-systems are often used in power transmitting. A system that can provide useful equations for this thesis may consist of two pulleys connected with a belt where one is driven by a motor, and the second is driven by the belts motion. This is called a belt transmission.

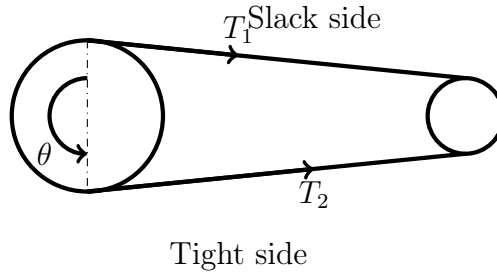


Figure 3.10: Drawing of a belt drive

The physics in equilibrium of the belt transmissions consists of two tension forces on both side of the pulley where one is bigger than the other, friction force resisting belt-slipping and a normal force from the belt resting on the pulley. Solving the equations for static equilibrium result in

$$\frac{T_2}{T_1} = e^{\mu \cdot \theta} \quad (3.9)$$

This equation is called the Capstan equation. It is not relevant for all belt transmissions, and it is highly dependent on the geometry of the belt. With different belt geometries the normal force, and thus the friction force subjected on the pulley will vary. Equation 3.9 is for a flat belt drive. There are different types of belt transmissions but the most common ones are flat belt drive and V-belt drive.

V-belt

The V-belts are usually molded in rubber, and are given their name due to the V-shape design of both the wedge and belt. The power transmission is done by wedging the rope in the V-shaped groove in the pulley, and transfer torque from the pulley to belt tension. [28]

The smaller the angle 2β is, the bigger the friction force is. This also leads to more wear due to friction and it also requires more force to get the belt out of the V-groove, which again leads to a loss of energy. Standard operating angle (2β) for a V-belt drive is therefore 32-38 degrees.[28]. When the belt is V-shaped the Capstan equation for flat belts does not hold. The relation between T_1 and T_2 is then

$$\ln\left(\frac{T_2}{T_1}\right) = \frac{\mu \cdot \theta}{\sin \beta} \quad (3.10)$$

By rearranging equation 3.10, an equation for the necessary friction coefficient μ can be obtained, depending on the tensions T_1 and T_2 , the contact angle θ and the groove angle β .

$$\mu = \frac{\ln\left(\frac{T_2}{T_1}\right) \cdot \sin \beta}{\theta} \quad (3.11)$$

From this equation it gets clearer why the friction force is greater when the groove angle, β , is smaller. The smaller β is the smaller $\sin \beta$, and thus the smaller coefficient of friction, μ , is necessary.

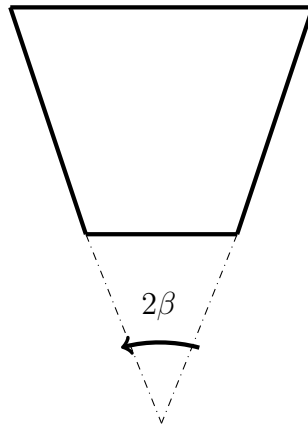


Figure 3.11: Cross-section of a V-belt

U-belt

U-shaped grooves are usually not used for power transmission. Given its geometry it is assumed that the force distribution around the groove is given by

$$N(\alpha) = N_{max} \cdot \sin \alpha \quad (3.12)$$

where N_{max} is the maximum normal force, α is the angle and $N(\alpha)$ is the force perpendicular to the surface at any point given α . An arbitrary value of α is drawn in figure 3.12 as an example.

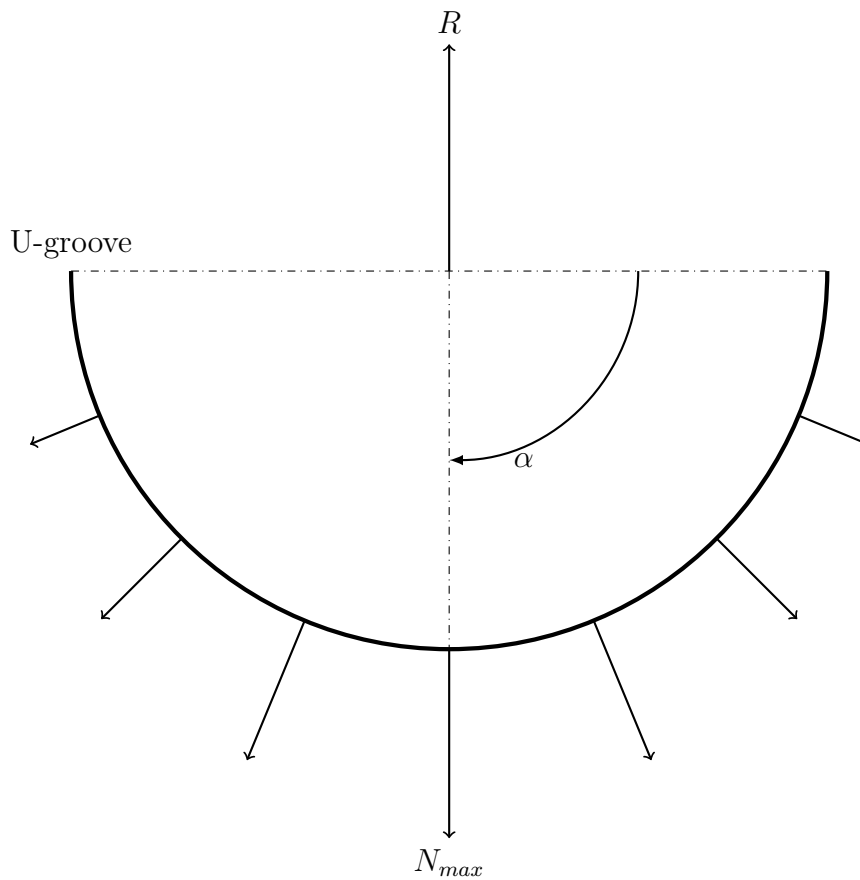


Figure 3.12: Force distribution in the U-groove.

Seen from figure 3.12, the normal force R is equal to the sum of all y-components of the vector field N . This means that

$$R = \sum N(\alpha) \cdot \sin \alpha = \sum N_{max} \cdot \sin^2 \alpha \quad (3.13)$$

Since this is a symmetric problem it follows that $0 \leq \alpha \leq \frac{\pi}{2}$. From this information, the following are obtained:

$$\begin{aligned} R &= 2 \cdot N_{max} \cdot \int_0^{\frac{\pi}{2}} \sin^2 \alpha \cdot d\alpha \\ &= 2 \cdot N_{max} \cdot \left[-\frac{\sin \alpha - 2 \cdot \alpha}{4} \right]_0^{\frac{\pi}{2}} = 2 \cdot N_{max} \cdot \frac{\pi}{4} \\ &\Rightarrow R = N_{max} \cdot \frac{\pi}{2} \end{aligned} \quad (3.14)$$

Using same method that was used to find the relation between T_1 and T_2 in the V-groove taking in account the equations

$$R = T \cdot d\theta \quad (3.15)$$

and

$$\begin{aligned} dT = f_s = \mu \cdot \sum N(\alpha) &= 2 \cdot \mu \cdot \int_0^{\frac{\pi}{2}} N_{max} \cdot \sin \alpha \cdot d\alpha \\ &= -2 \cdot \mu \cdot N_{max} \cdot [\cos(\alpha)]_0^{\frac{\pi}{2}} \\ &\Rightarrow dT = 2 \cdot \mu \cdot N_{max} \end{aligned} \quad (3.16)$$

The following are obtained:

$$\ln \frac{T_2}{T_1} = \frac{4 \cdot \mu \theta}{\pi} \quad (3.17)$$

Rearranging the factors to find a expression for μ

$$\mu = \frac{\ln \frac{T_2}{T_1} \cdot \pi}{4\theta} \quad (3.18)$$

3.5 Properties of rubber

3.5.1 Poisson's Ratio

Poisson's Ratio is the ratio which describes how a material deforms in the direction perpendicular to the load-direction. Most of the materials found in nature have a Poisson's ratio between 0 and 0.5. The Poisson's Ratio is defined as: $\nu = -\varepsilon_{Lateral}/\varepsilon_{Axial}$. While most metals have a Poisson's ratio at about 0.3, most rubber materials have a Poisson's ratio very close up to 0.5. This means that most rubber materials have a volumetric strain equal to zero, meaning that the material is nearly incompressible, a fact that is very important when considering the stress-strain relationship of the tether when it is compressed.

3.5.2 Young's Modulus

Young's Modulus, also called the modulus of elasticity, is a property in material mechanics which describe the tensile stiffness of a material. The Young's modulus for many materials are defined as: $E = \sigma/\varepsilon$.

From the all so familiar stress-strain curve, the Young's Modulus defines the slope of the linear area of the curve in the elastic part. A high Young's Modulus describes a stiff material, and a low Young's Modulus conversely describes a less stiff material.

Non-linear elasticity area

For most materials the Young's Modulus is a very useful property as it measures the material's stiffness. For the Young's modulus to be a constant value for a given material, the elastic part of the stress-strain curve has to be linear. This is however not the case for all materials. This is neither the case for rubber-materials, which are not elastic, but viscoelastic materials. Finding a single Young's Modulus that is valid for the entire elastic region of viscoelastic materials is not possible, as the stiffness of the material depends on the stress-rate, which in the viscoelastic case is not constant. The value therefore have to be estimated inside intervals.

Compressive vs tensile stress

The modulus of elasticity of a material explains how the material reacts under different loads that are in the elastic area. These loads may be tensile, compressive or torsional, and the material therefore has different moduli for the different scenarios. Many materials, especially metallic materials, have

somewhat constant modulus of elasticity and the value is more or less unchanged for the different forces that can be applied. On the other hand, there are many materials that behave differently under various loading scenarios. Rubber is one of these substances. The rubber materials may often be able to elastically deform by many times its own original length under tensile stress, but behave very differently to compression. The compression modulus and the tensile modulus therefore differ greatly in such a material. Typically, the compression modulus of any elastomeric material is larger than the tensile modulus, which means that more force is required to elastically compress the material than what is required to elastically elongate the material.

Hysteresis

The phenomenon hysteresis is present in rubber materials, meaning that when rubber is, for example, compressed then decompressed, the strain of the material during compression equals the deformation during the decompression, but the stress subjected is not the same.[32] The phenomenon can be described by a stress-strain curve seen in figure 3.13. The two different stress-strain curves from loading and unloading represents energy loss in form of heat. In normal elastic materials a cyclic load does not result in energy loss in the elastic region, but this is not the case for viscoelastic materials due to rearranging of the molecules causing heat and energy loss.

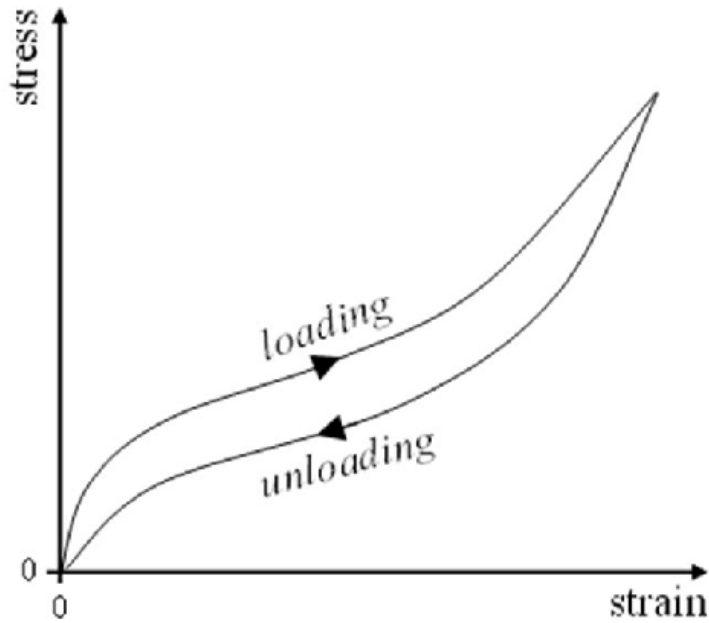


Figure 3.13: Hysteresis described by a stress-strain curve.[31]

3.5.3 Treloar's Equations - SIF

While compressing rubber materials, one will experience that as the material deforms it gets harder and harder to compress it further. This makes sense as pulling a rubber band to 100% of its length may be easy, but compressing it up to 100% of its thickness is practically impossible. There must therefore be a factor that says something about how much the amount of compression will increase the force required to compress the material further. There have been conducted some research on this topic, and one of the people that have been most influential is L.R.G. Treloar and his work “The physics of rubber elasticity” from 1975[35]. Treloar created some general equations that estimate the increasing resistance during elastic deformation of elastomers. Treloars findings have been refined further, and in the paper “An analysis of rubber under strain from an engineering perspective” written by Daniel L. Hertz Jr. in 1991 [19], the author provide the relation between compression and increasing internal stress equivalents. The relation is called the stress intensification factor and is given by:

$$SIF = \gamma - \gamma^{-2} \tag{3.19}$$

Where γ is the new desired thickness of the material. For instance if the material should be compressed to 0.7 of its original height, the SIF would

be about -1.34. This means that the compressive force required to compress the material to a height of 0.7 of the original height, must overcome an additional internal force of 1.34 times the force that is given from hooks law. For instance, if the force required to compress a material to 0.7 of its original height according to hooks law is 10 MPa, the SIF says that an additional 13.4MPa is needed to compress the material to the desired thickness. This means a total of 23.4 MPa would be needed to compress the material to 0.7 of the original thickness. The SIF model is especially accurate for all non-crosslinked, unfilled elastomers, but it is believed that it will be able to give a more accurate description of the forces required to deform any elastomeric material.

3.5.4 Frictional and wear properties of rubber

Frictional properties

Friction properties of rubber are quite complicated properties to obtain that includes many factors within chemistry and physics. When in contact with a surface, rubber form adhesive forces.[16] These forces are described as the substance's ability to stay attached to the other surface. Water that stays on the surface on the inside of a glass is an example for where adhesive forces can be found.[34] The same happen for substances like rubber when in contact with other surfaces. Adhesive forces and forces due to hysteresis are two factors that contributes to the frictional forces between a rubber and a hard surface.[16] Hardness is also a factor when it comes to the coefficient of friction. From a study of shoe soles' increase in friction it was roughly estimated that the coefficient of friction between the sole and the floor was around 1 for hardness between Shore A 65 and Shore A 75, and 0.5 for Shore A 85 and above.[22] Though it is unclear how valid this is for other types of rubber, one can see a connection between the hardness of the material and the adhesive forces in the works. Harder material will experience less contact area which means lower adhesive forces, which again affects the coefficient of friction.[16] A study was conducted about the content of PVC composites (polyvinyl chloride) in NBR (acrylonitril butadiene rubber) and how it affects the friction and wear. The tests consisted of testing at different PVC concentration in the mixture. As the PVC concentration increased, the hardness also increased and the coefficient of friction decreased.[16]

Wear properties

One thing to consider when choosing the right rubber for a given situation is to make sure that the elastomer does not get worn down extensively over time. When exposing an elastomer to frictional forces its surface can start to get worn down if the wear properties of the rubber is not sufficient for the load that it's exposed to. As for frictional properties, this is a very complex set of properties which relies on many different factors.[16] There are several important aspects to consider when looking at the lifespan of rubber. Compression set is one of them. Compression set is the everlasting deformation of a material when compressed at an exact deformation for a set duration of time at a predetermined temperature[21], and is found experimentally[8]. Another factor often considered when dealing with rubber is creep. Creep is defined as the permanent deformation over time when exposed to stress.[21] Hardness of the rubber also have an impact of the wear. In the same study of NBR with content of PVC, as the hardness increased, the wear rate decreased. [16] Although the hardness has an effect on the wear it is important to understand that hardness is only one factor that affects wear, and therefore one should be careful to determine the wear from this information only.[33] Abrasion resistance is a quality often considered when using rubber, and is defined as a surface's ability to prevent wear.[29] Abrasion resistance is a very complicated attribute that are influenced by, among others, tear strength, the friction coefficient, resilience and heat dissipation.[10] Depending on the rubber material, these properties can vary greatly[8], and these attributes may be enhanced by inserting additives.[26]

3.6 Drum

3.6.1 Lebus Shell

As previously mentioned, the current design of the M-TMS is equipped with a unit called the Lebus Shell. Figure 3.14 shows a general layout of the current solution of the drum on the M-TMS. The tether enters the drum on the bottom of the left side end filler. The tether then follows the trajectory made from the grooves. When the tether is spooled all the way to the other side, there are end fillers there to make the tether lay neatly on top of the previous layer. These end fillers are usually welded with precision to obtain the tether behaviour wanted while moving from

one layer to the next. When spooling back to the other side, the end filler again makes sure that the tether is placed on top of the previous layer. In this layout the tether lays parallel to the flange except for the part in Figure 3.14 which is labeled the crossover section. Each crossover section makes the tether go across the drum with a half pitch each, causing a needed full pitch in each revolution. After the initial layer, the tether itself makes up the trajectory for the placement of further layers on top. The consecutive layers will lay themselves in between the wedges, and only cross over the tether underneath in the crossover sections made up of the grooves on the drum. This setup allows for controlled spooling, and less tether damage as the tether only crosses over the previous layer in two crossover sections per revolution in a controlled manner. [12]

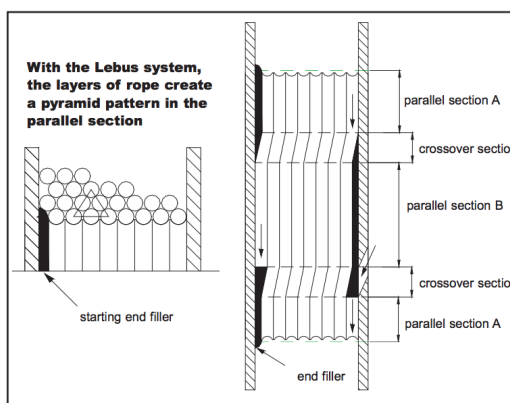


Figure 3.14: Layout of the Lebus Shell. [12]

3.6.2 Tension during spooling

As mentioned earlier, it is important for the tether to be spooled on the drum with tension. If this is not done, slack can be developed in the cable. After further spooling of tether on the drum this slack cable could then be crushed because of the improper placement, causing an undesirable tether replacement. According to the market leader in wire spooling technology, Lebus, the tension should be at least 2% of the breaking load or 10% of the working load when the system is equipped with a Lebus drum. [12] The calibration of the electrical motors on the drum and the tension wheel is done to accommodate that this tension is always present when winding the tether.

3.6.3 Fleet angle

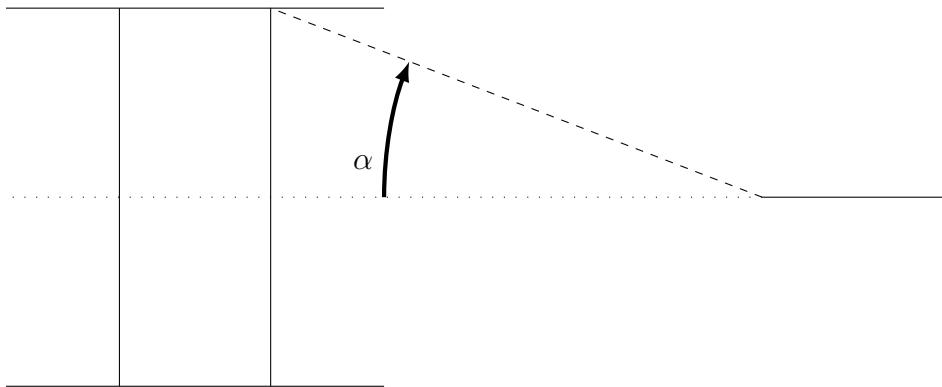


Figure 3.15: Illustration of the fleet angle

The fleet angle is defined as the largest angle between the center line of the drum and the tether on the drum, with the pivot point of the angle being the sheave closest connected to the drum, as shown Figure 3.15. The optimal fleet angle very much depends on the drum and cable configuration, but according to Lebus the fleet angle should be no more than 1.5 degrees, and not less than 0.25 degrees when using the Lebus shell layout. [12] This is desirable to make sure the cable is placed properly on the drum, in addition to the tether not climbing out of the sheave groove. .

3.6.4 Fleet angle compensators

In many constructions it is easy to place the sheave further or closer to the drum to get optimal fleet angle for spooling, but this is not the case for a number of designs, including the M-TMS. In the M-TMS the design is made as compact as possible to reduce drag during operation. It is therefore not possible to place the support wheel closest to the drum far enough from the drum to obtain desirable fleet angle (visualized in Figure 2.2). To accommodate this problem, a fleet angle compensator is added. This is a unit that moves across the drum between the flanges, continuously making sure that the flange angle is inside the desired area during spooling.

Screw level winder

There are multiple types of fleet angle compensators, but in the M-TMS, IKM have opted for a screw level winder. The screw level winder consist of a self reversing screw shaft upon which a component with rollers are mounted. The screw shaft is connected to an electrical motor which makes the shaft rotate, causing the rollers to move between the flanges of the drum and effectively provide the system with the appropriate fleet angle.

3.7 Contact stress calculation

The stress between the tension wheel and the tether can be calculated using a series of formulas provided by our supervisor, professor Dimitrios Pavlou. The equations are used in some of the subjects he teaches, and they are based on the works "Advanced Mechanics of Materials"[1]. The equations use material and geometric coefficients of the bodies in contact, and typically require input such as contact force or contact pressure to calculate for instance the deformation of the materials. In this case the relation is flipped and one wants to calculate how much contact pressure a certain deflection corresponds to. One can use this output to calculate the contact force between the two bodies. In the case of the tension wheel and tether, one can consider the tension wheel a thin disc in contact with a thin box, where the height is from the centre of the tether and out to the point of contact with the tension wheel. Then one can simply integrate the values of contact force around the circumference of the tether to achieve valid values of contact force of the whole surface. This can be considered the normal force, which again can be used to calculate what friction coefficient is necessary for operation. The geometric coefficients A and B determines how the deformation of the bodies in contact behave. The geometric coefficient are determined by the radii of the objects along different axis, and figure 3.16 is used to visualize the relevant radii of the bodies in the case mentioned above. Δ can be viewed as a constant concerning the materials in contact, where both the geometric (A and B) and the material specific (ν and E) coefficients are factors. The equations that follow use b and W as factors, where b is the width of the indentation, and W is the distributed contact force (N/mm). The stress can then be calculated. As mentioned, all equations below are collected from professor Dimitrios Pavlou's lecture notes.

$$A = \frac{1}{4} \left(\frac{1}{R_1} + \frac{1}{R_2} + \frac{1}{R'_1} + \frac{1}{R'_2} \right) - \frac{1}{4} \left(\frac{1}{R_1} - \frac{1}{R'_1} + \frac{1}{R_2} - \frac{1}{R'_2} \right) \quad (3.20)$$

$$B = \frac{1}{4} \left(\frac{1}{R_1} + \frac{1}{R_2} + \frac{1}{R'_1} + \frac{1}{R'_2} \right) + \frac{1}{4} \left(\frac{1}{R_1} - \frac{1}{R'_1} + \frac{1}{R_2} - \frac{1}{R'_2} \right) \quad (3.21)$$

$$\Delta = \frac{1}{A + B} \left[\frac{1 - \nu_1^2}{E_1} + \frac{1 - \nu_2^2}{E_2} \right] \quad (3.22)$$

$$b = \sqrt{\frac{2 \cdot W \cdot \Delta}{\pi}} \quad (3.23)$$

$$\sigma_{max} = -\frac{b}{\Delta} \quad (3.24)$$

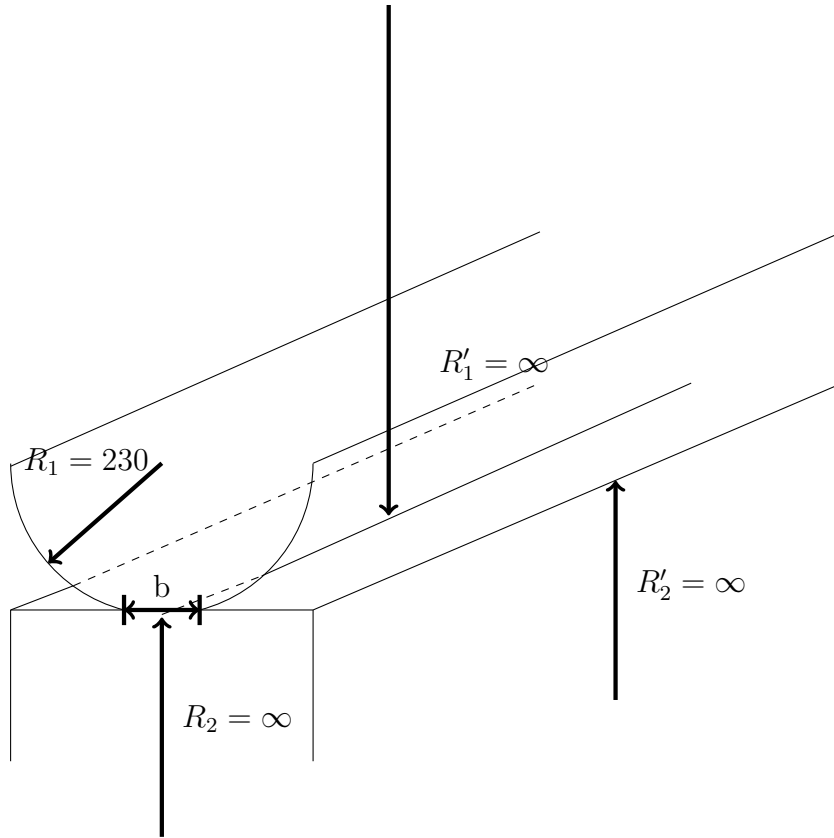


Figure 3.16: Visualization of relevant radii for contact stress calculation

Chapter 4

Assumptions

Since this is a strictly theoretical thesis, a fair amount of assumptions has been made to make the calculations both less complicated and doable. For further analysis it is recommended to induce testing in similar conditions as for the area of use.

4.1 Capstan equation

For use of the Capstan equation it is necessary that some conditions are fulfilled. The tether is on the brink of slipping. That means that the static friction force, f_s , is at its maximum potential. The capstan equation only works for non-rigid bodies. Since the tether clearly is not rigid, this is fulfilled. The last condition is that the tether must be non-elastic, which it is not. But, since the loads are mostly in the axial direction, and the aramid yarn will stop the deformation with loads present in this direction, it is assumed that the tether is non-elastic, meaning that the tether will not stretch to any measurable extent, for this purpose. [37]

4.1.1 U-shaped groove

Considering lack of good models, it is assumed that the force distribution along the U-shaped groove is $F(\alpha) = F_{max} \cdot \sin \alpha$, where $0 \leq \alpha \leq \pi$.

4.2 Tether squeezing limit

In order to be able to calculate how squeezing will affect the tether, some assumptions about the materials in question is necessary. The tether consists of multiple layers of different materials with different properties. These assumptions, as well as a description of the different layers of the tether, will be further discussed and explained in the analysis.

- The thermoplastic rubber, the outer rubber sheet on the tether, has a compressive modulus of elasticity of around 4.1 MPa (Assumption based on tensile-stress data from Nexans, the producer of the tether).
- The aramid armouring yarn will not compress to any measurable extent.
- The thin inner sheet of polyethylene will not compress to any measurable extent.
- The majority of the difference in tether diameter is due to difference in the outer TPR layer
- The tension wheel will not compress to any measurable extent.
- The outer sheet of thermoplastic rubber is considered incompressible, as most rubbers without air-pockets are approximated to be. This includes having a Poisson's ratio of 0.5 meaning that the material volume is always conserved.

These assumptions allow for the focus to be on the outer protective layer on the tether, and this is where the deformation will take place.

4.3 Data from IKM

The data retrieved from IKM are non-exact. The forces displayed in the analysis are not necessarily the actual forces working on the system. The data used in the thesis are estimated to be the maximum loads, and therefore the results follow these "worst case" scenarios. It is therefore assumed that the energy lost in the support wheels, spool and by the environment are negligible. The used data that are assumed are:

- During rewinding: $T_2 = 350kg$ and $T_1 = 100kg$
- During unwinding: $T_2 = 300kg$ and $T_1 = \frac{T_2}{10}$

T_1 can, in theory, be totally slack in the unwinding process, so the tension force on the outer part of the TMS could be 0. Since this causes a big problem in calculating the necessary friction coefficient it is assumed that the tension force on the outer part of the TMS, T_1 , is equal to $\frac{T_2}{10}$, such that Capstan equation can be used to solve this problem.

4.4 Material choice

Since there are limited information about rubber mixtures, assumptions have been made when it comes to the tables picked for comparisons of rubber (figure 5.11, figure 5.13, figure 5.14). It must be taken into account that rubber is a very versatile material that varies a lot. Without the proper data from testing it is a possibility that the rubber materials excluded from the aforementioned tables is a good fit for the tension wheel of the TMS.

Chapter 5

Analysis and discussion

IKM has experienced several issues with the TMS design. The main hurdle is the z-kink issue. When the z-kink issues arise extra expenses in the form of purchasing new tethers, extra man-hours and TMS downtime follow. To find a solution to minimize these expenses are therefore in IKM's best interest. Material suggestions to optimize the TMS and lifespan is another subject that will be discussed, as this is also a part of the minimization of material and labour costs. The last issue that is analyzed in the following chapter is the possibility of getting rid of the Lebus-shell. The shell is an expensive unit, and being able to operate without it is therefore a way to save time and money. To summarize, the following analysis will go in depth on the following issues:

- What causes the z-kinks in the TMS?
What solutions can be applied?
What new issues/limitations do the solution lead to?
- Can new material choices improve the TMS performance and how?
- Can one avoid using the Lebus-sheel in the TMS and how?

5.1 Z-kink issues

Source of the z-kink issues

The problems related to the M-TMS is, as stated in the introduction, the formation of z-kinks in the tether. The engineers working to resolve this issue has some theories of what is the cause of the z-kinks, and they have also considered a few solutions to the problems. The design will be broken down, in order to gain an understanding of what forces are present, and what forces are required to create a z-kink in the first place.

Z-kinks are present where a cable's conductors have been elongated, and the cable is released from tension. This allows the cable to go back to its original length, while the conductor is elongated, creating the z-kink. Forces in the M-TMS that may cause this are:

- Axial tension
- Radial compression
- Bending over small diameters

The tether is to some extent exposed to all these situations in the M-TMS, and it will be analyzed how much the tether is affected by the different forces.

Axial tension

The tether is in axial tension during the rewinding and unwinding of the drum. This tension provides controlled winding of the tether, and is in a magnitude of up to 350 kilograms of force. The tether used in the M-TMS is the RT-618 produced by Nexans. The data sheet of this tether says that the tension at conductor yield is 65kN. This equals a tension of about 6625 kg of force. This indicates that the axial tension the tether is exposed to during operation, is close to insignificant. This means that axial tension alone can be ruled out of being the cause of the z-kinks seen in the tether.

Bending over small diameters

When a cable of any sort is bent around a small enough diameter, the state of compression and tension inside the cable is large enough to damage the conductors. The part of the cable closest to the centre of bending will be in a state of compression, and the outer part of the cable furthest away from the centre of bending will be in tension. This alone might be enough to cause the state of the conductors to exceed the yield strength and cause z-kinks or other cable damage.

The RT-618 datasheet gives a minimum dynamic bending diameter at 1200mm. The smallest bend of tether in the M-TMS is 460mm. This is a lot tighter than the recommended minimum bending diameter, and one might therefore head to the conclusion that this is the cause of the problem with z-kinks. However, data from Nexans own tests of the tether provided by IKM tell a different story. Nexans engineers did a series of tests where they cycled the RT-618 around a 400mm bend under different loads. They first cycled the tether over the bend 500 times at a load of 5kN, which equals about 510 kg of force. They then cycled the tether 25 times at a 12kN tension, which equals about 1220 kg of force. The examination of the tether showed no sign of z-kinks or other damage. The fact that the tests were conducted without damage at a smaller bending diameter, and also at greater tether tension than the M-TMS experience is a sign that the bending of the tether is unrelated to the z-kinks.

Also worth noting is that the forces created by bending is at a maximum on the outermost part of the tether. If this was the cause of damage, one would experience the most cable damage at the outermost conductors in the tether. However, it is observed that the z-kink issue is mainly a problem for the innermost conductors. For this reason as well as the bending tests Nexans have conducted, bending over small diameters can be ruled out as the main cause of z-kinks.

Radial compression

The engineers at IKM believes that squeezing is the main source of the z-kinks that are seen in the tether. By squeezing one is referring to radial compression from all around the cable, giving it little to no room to move freely into. The M-TMS are as stated designed with multiple wheels throughout the tethers trajectory. The final support wheel and the tension wheel are situated next to one another. The wheels have a v-shaped groove that is the contact surface with the tether. The fact that these two wheels are so close to one another means that the only gap between them is the hole created by the to v-shaped grooves. The cross sectional area of this gap is in total smaller then the cross sectional area of the tether itself. This is what is believed to be the source of the z-kinks. In order for the cable to get through the gap, something must deform to some extent.

A positive effect of having a tight fit between the tension and support wheel is the fact that sufficient friction force is easily achieved. The tight fit will induce a normal force between the tether and tension wheel that is large

compared to a scenario with no squeeze, and this allows for a material with lower friction coefficients or worn tension wheel surface to be used. This is given by the fact that the force of friction is set as the product of friction coefficient between the surfaces and the normal force. The large increase in normal force allows for an equally large drop in friction coefficients.

5.2 Evaluating the different solutions to the z-kink problem

Following is the analysis of operating the TMS using V-shaped tension wheel and a U-shaped tension wheel with no squeeze. Then, the squeezing situation is considered, where a squeezing limit and a calculation of necessary squeezing to operate TMS safely is calculated.

To get a better overview of the different shapes that are relevant, the U-shape and the V-shape, it is important to do the calculations on how these shapes affect the friction if there would be no squeezing involved. Another reason for these calculations is the fact that the tether diameter is $37,4mm \pm 1mm$, so even if there was to be some squeeze there might be a distance where the diameter is smaller than $37,4mm$, causing a no squeeze situation.

Figure 5.1 and 5.2 shows the free body diagrams of the situations and the forces in play in the system. The gap between the tension wheel and closest support wheel is exaggerated for visualization purposes.

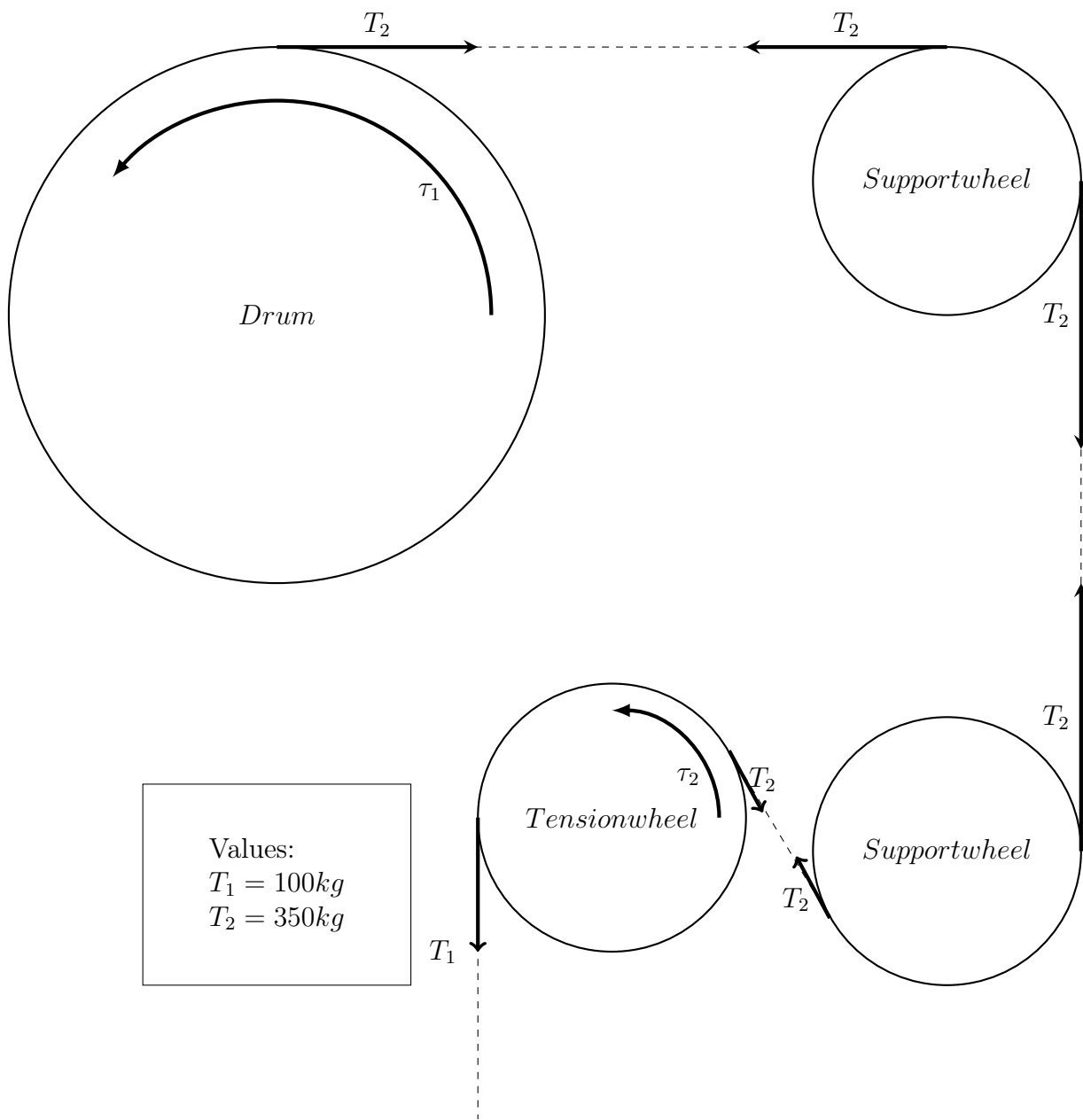


Figure 5.1: Free body diagram during rewinding.

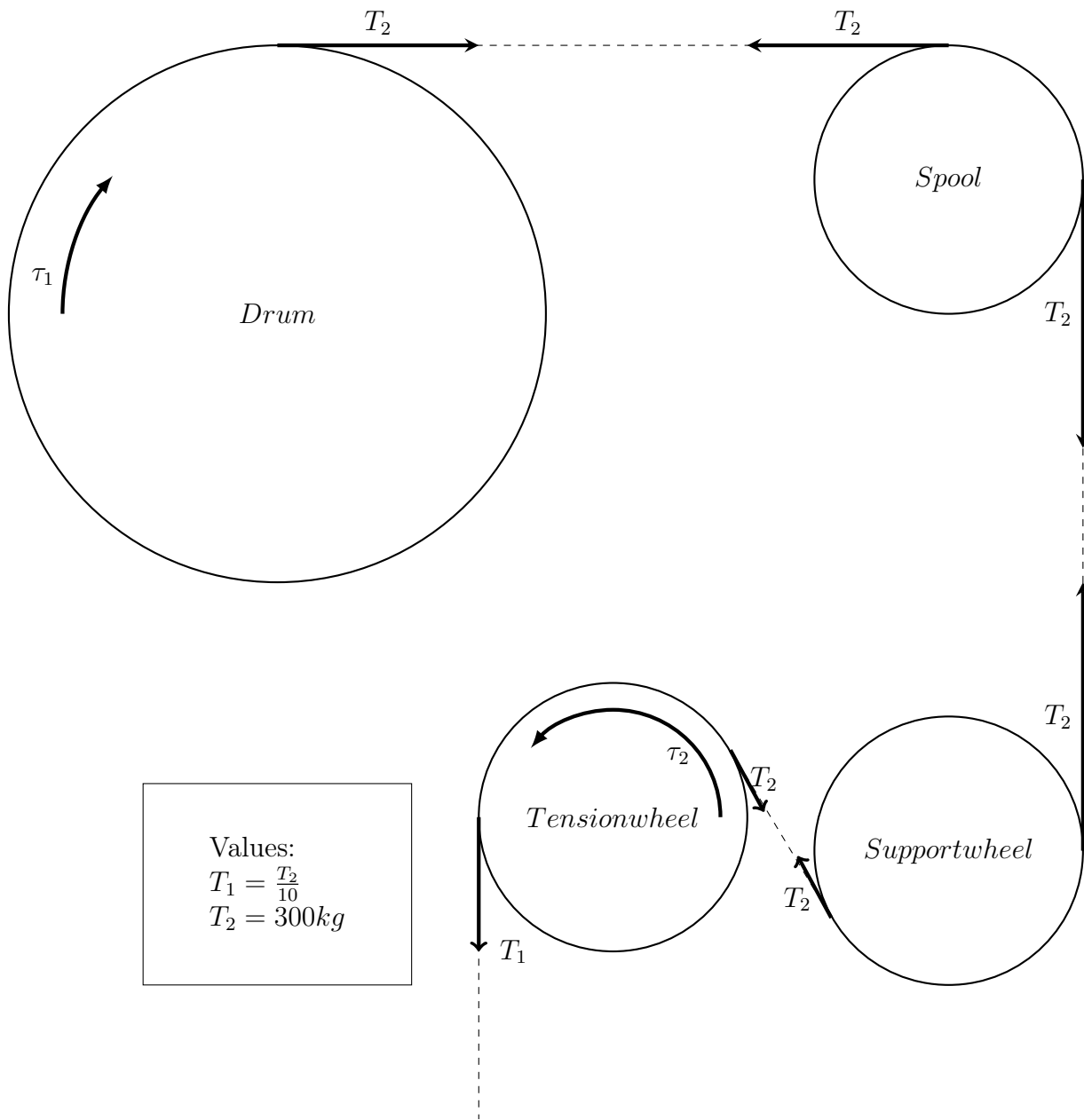


Figure 5.2: Free body diagram of unwinding.

Looking at figure 5.3, the Merlin TMS contact angle θ is equal to 144.5 degrees. During rewinding, the two tension forces are $T_1 = 100kg, T_2 = 350kg$ and during unwinding it is assumed that $T_1 = \frac{T_2}{10}$ and $T_2 = 300kg$. This section describes what the necessary coefficient of frictions would be for both

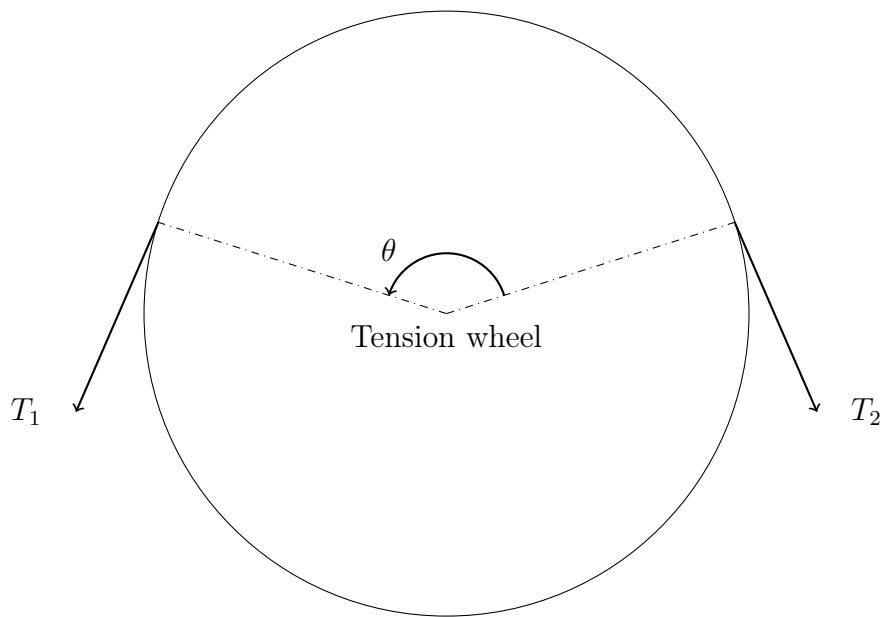


Figure 5.3: Visualization of tension wheel.

unwinding and rewinding of the tether in a situation where there would be a V-shaped or U-shaped tension wheel with no squeezing. To get a clear picture, the four scenarios with rewinding and unwinding for both V-shaped and U-shaped groove has to be looked at closely. These scenarios assumes that there would not be any squeeze and thus no damage due to squeezing on the tether. When there is no squeeze the friction forces originates from the tension in the tether. Comparing it to a power transmission system, equations from chapter 3.4 can be used.

During rewinding the tension wheel runs what IKM calls "speed mode". This means that while the drum pulls the tether at 350kg, the tension wheel is provided a torque such that the tether moves out at either 0.3m/s or 0.6m/s. During rewinding, the drum applies all the tension in the tether between the drum and tension wheel.

IKM's values from unwinding the tether shows that the tension wheel pulls the tether out with a force of up to 300kg. The corresponding tension in the tether between the tension wheel and the lowest support wheel would then be 300kg. Since the tether is being pulled out there is not necessarily any tension in the tether on the other side of the tension wheel, the part between the tension wheel and ROV.

5.2.1 V-shape with no squeeze

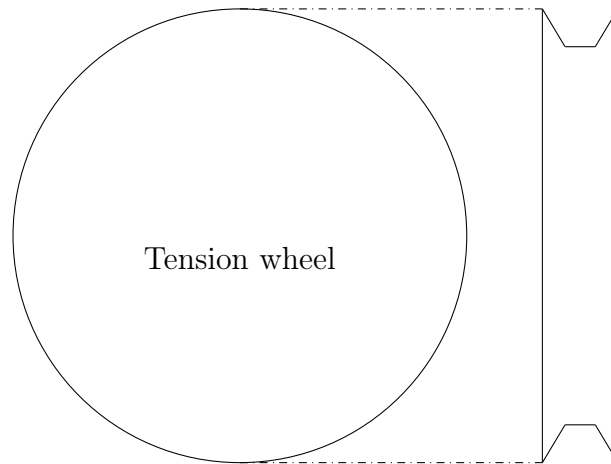


Figure 5.4: V-shaped tension wheel. This figure is not up to scale of the actual tension wheel

Rewinding

The values from IKM is showing that in the rewinding process the drum pulls the tether, at the highest, with 350kg, the corresponding tension in the teher between the tension wheel and ROV is 100kg. IKM's drawings of the tension wheel shows that $\beta = 30^\circ$, and finally the contact angle of the tether is $\theta = 144.5^\circ$ Using equation 3.10 the corresponding friction coefficient is obtained. μ must be

$$\mu \approx 0.25$$

Unwinding

Assuming that $T_1 = \frac{T_2}{10}$, one can obtain the necessary friction coefficient, μ , in the unwinding process. Since $T_2 = 300kg$, in this instance this means that $T_1 = 30kg$. Plugging in the numbers in 3.10 the necessary friction coefficient is

$$\mu \approx 0.46$$

5.2.2 U-shape with no squeeze

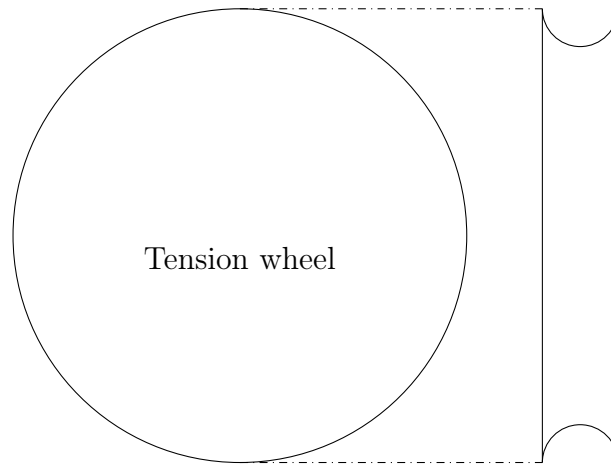


Figure 5.5: U-shaped tension wheel. This figure is not up to scale of the actual tension wheel

Taking equation 3.18 into account, one can get the value for the necessary friction coefficient, μ , between the tether and the tension wheel to wind the tether without slips for the U-grooved design.

Rewinding

With the values, $T_1 = 100kg$ and $T_2 = 350kg$, $\theta = 144.5^\circ$ the following is obtained from equation 3.18:

$$\mu \approx 0.39$$

Unwinding

Assuming again that $T_1 = \frac{T_2}{10}$ one gets the necessary friction coefficient from 3.18 to be

$$\mu \approx 0.72$$

5.2.3 Considerations of the no-squeeze design

One alteration that could be made when considering the no-squeeze design is to try to alter it to get a larger contact angle θ . By increasing the contact angle one would effectively need a smaller friction coefficient to operate the unit. However, the assumption $T_1 = \frac{T_2}{10}$ might not be valid for all stages during operation. For instance, the ROV might stop for a second, and the load T_1 might become a lot smaller and even disappear for some time. If T_1 becomes very small, the necessary friction coefficient needed without squeeze will increase immensely, no matter the contact angle. If the outboard force goes to zero, the necessary frictional coefficient goes to infinity, according to the Capstan equation. For this reason, it is believed that a solution that is not dependant on outboard tether tension is preferred. The solution that is suggested is using a U-shaped groove with a slightly smaller diameter than the tether itself, providing some squeeze. This will ensure a minimum normal force between the tether and wheels, and by that a constant value of minimum necessary friction coefficient.

5.2.4 Squeezing limit

Introduction and implementation of assumptions

The cable has, as stated previously, been subjected to squeezing which is believed to be the main cause of the z-kinks problem. The squeezing does however provide a large normal force between the tether and the tension wheel, which again enables there to be a sufficient frictional force between the surfaces. This frictional force is what allows the tension wheel to convert its torque to pulling force on the tether. The squeezing therefore is both a useful feature, at the same time as it is one of the reasons the TMS is experiencing issues. One of the most important questions this rises, is then how much squeezing can possibly be allowed to happen while keeping all the conductors inside the tether free of damage. In this case it is considered the wheels have U-shaped grooves that squeeze the cable equally around the tether circumference.

The tethers cross section is a complicated material composition. The outer sheet is made of a TPR, or a thermoplastic rubber. Only some of the specific material properties of this material are known, the unknown properties can be estimated to some degree of accuracy. Inside the outermost sheet is the armouring yarn of the tether. The tether RT-618 has an armouring yarn made of aramid, which is commonly associated with being used in Kevlar. The aramid armouring is made up of fibres. Inside the armouring yarn lays the inner sheet, which is made of polyethylene. Polyethylene is a versatile material, but one may assume there is used some form of low density polyethylene (LDPE), as the tether is flexible to some degree. This flexibility would not be achieved if there was high density polyethylene(HDPE) in the tether. Inside of the inner layer there are multiple layers of different conductors. There are power conductors and fibre optic elements placed in three different layers. The conductors are insulated with a thin polyethylene insulator. The layers are separated using some form of tape, and each layer is filled out with a filler compound that prohibits large air bubbles and wiggle-room for the conductors.

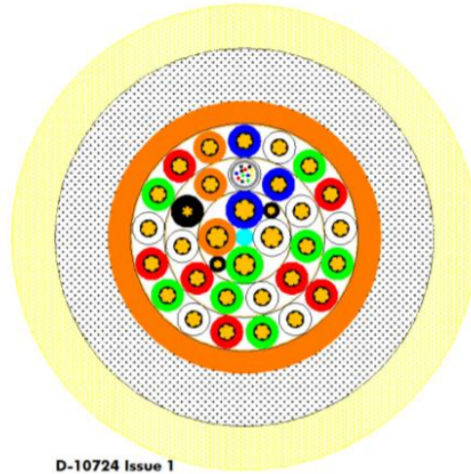


Figure 5.6: Cross section of Nexans RT-618 tether. Illustration provided by Nexans

When modelling how the squeezing affects the cables, one must do some assumptions. The assumptions will affect the final results, and one may argue that this is not accurate enough for it to be considered realistic. The assumptions are however quite conservative, and the values found are believed to be accurate enough as an approximate value. When there is a lack of proper data to be found and experiments are not conducted to find accurate representations, one may only find good approximations. The assumptions and approximations are, as previously mentioned, as follows:

- The thermoplastic rubber has a compressive modulus of elasticity of around 4.1 MPa (Assumption based on tensile-stress data from Nexans, the producer of the tether).
- The aramid armouring yarn will not compress to any measurable extent.
- The thin inner sheet of polyethylene will not compress to any measurable extent.
- The majority of the difference in tether diameter is due to difference in the outer TPR layer
- The tension wheel will not compress to any measurable extent.
- The outer sheet of thermoplastic rubber is considered incompressible, as most rubbers without air-pockets are approximated to be. This includes having a Poisson's ratio of 0.5 meaning that the material volume is always conserved.

These assumptions allow for the tether to be considered as a two material system when it comes to the squeezing problems. The tension wheel is not considered to deform, as the task is to figure out how much the tether itself can be squeezed without damage. The parts considered in the calculations are therefore the outer sheet and the core (the armouring, the inner sheet and the conductors). This means that the outer sheet will be deforming, and everything inside the outer sheet, the core, will not be compressed to any measurable extent. The maximum pressure that will be allowed to affect the core will therefore be the yield strength of the copper conductors. The compressive yield strength of copper is said to usually be around 45 MPa [3], and the pressure in the core must for that reason never exceed this value of 45 MPa.

Calculation of squeezing limit

Using the equations from the contact stress theory, as well as the stress intensification factor (SIF), one can calculate how different depths of indentation corresponds to different stresses in the TPR material. In this case the variable γ from the SIF is considered to be $\left(1 - \frac{\delta}{t}\right)$. The SIF will be directly added as a factor of increased stress, in this case negative due to compression, and using this together with equation 3.24, one will end up with the following equation.

$$\begin{aligned}\sigma_{max} &= -\frac{b}{\Delta} \cdot (1 - SIF) \\ \sigma_{max} &= -\frac{b}{\Delta} \cdot \left(\frac{\delta}{t} + \left(1 - \frac{\delta}{t}\right)^{-2}\right)\end{aligned}\quad (5.1)$$

The coefficient b in the above equation can be expressed using Pythagoras's relation of right angled triangles. As shown in figure 5.7. This gives the following relation for the variable b .

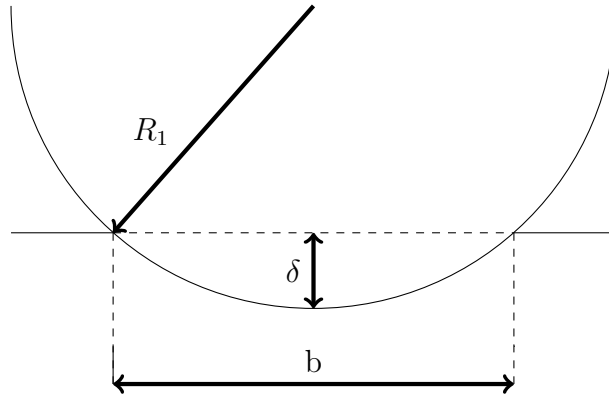


Figure 5.7: Visualization of coefficients δ and b

$$b = 2 \cdot \sqrt{R_1^2 - (R_1 - \delta)^2} \quad (5.2)$$

Now one must calculate the Δ factor using equation 3.22. In this case R_1 , the radius of the tension wheel, is the only coefficient that is not approximated to be ∞ , and is given to be 230mm. The first factor of the equation is therefore:

$$\frac{1}{A + B} = \frac{1}{\frac{1}{2 \cdot R_1}} = 2 \cdot R_1$$

The rest of the Δ expression is given using material coefficients. The material coefficients in question are the compressive modulus of elasticity for both materials, as well as Poisson's ratio. Given that one assumption is that all of the compression is done by the TPR layer of the tether, the compressive modulus of the tension wheel may therefore be assumed to be very large. In that case, the factor using this number, E_2 , is negligible. The material coefficients of the TPR material are previously assumed to be $E_1 = 4.1MPa$ and $\nu = 0.5$. The calculation of Δ , which will be valid for all values of deformation, is then as follows.

$$\Delta = 2 \cdot R_1 \cdot \left(\frac{1 - 0.5^2}{4.1} \right) = 84.15 \frac{mm^3}{N}$$

One will now end up with the following equation for the stress using the deflection as the only unknown variable.

$$\sigma_{max} = -\frac{2 \cdot \sqrt{R_1^2 - (R_1 - \delta)^2}}{\Delta} \cdot \left(\frac{\delta}{t} + \left(1 - \frac{\delta}{t} \right)^{-2} \right) \quad (5.3)$$

To calculate the indentation at a given maximum stress, one would need to decide on a maximum stress and a sheet thickness. In the following calculations the maximum stress is set to an example value of 20MPa. The thickness of the TPR sheet is set to its nominal thickness of 3.5mm, which is given from the tether producer Nexans. This would according to equation 5.3 correspond to a maximum indentation of $\delta = 2.77mm$. One could compare this to the indentation at the absolute maximum stress, which in this case is 45MPa, the compressive yield strength of copper. If one considers the nominal tether diameter, which means the sheet thickness is 3.5mm, putting this into equation 5.3 one would get an indentation of $\approx 3mm$ maximum. This shows that more than a doubling of stress only allows for about 10% more strain. This means that there are small margins for error when getting close to the maximum stress, and small diameter differences may cause large stress concentrations. For this reason, the stress of 20MPa is used for some of the further examples.

To conclude on an accurate squeezing limit will in this case be difficult, as important material coefficients are uncertain. The equations should however be valid to some extent, and if tests are conducted to find the material coefficients one could use these to find a more accurate squeezing limit. For instance the TPR could be more plastic-like in behaviour and have a larger modulus of compression, this would again lead to less compression being allowed. Therefore the numbers obtained are considered an approximation and suggestion only, and further testing should be conducted.

Calculation of normal force and friction coefficient

From the theory about contact stresses, equation 3.23 and the previously shown equation 5.2 can be used. Setting these two equations for coefficient b equal will result in the following relation.

$$b = \sqrt{\frac{2 \cdot W \cdot \Delta}{\pi}} = 2 \cdot \sqrt{R_1^2 - (R_1 - \delta)^2}$$

This relation can then be solved for coefficient W , which is the amount of contact force per unit length $\left[\frac{N}{mm}\right]$. Solving the relation for W will lead to the following equation.

$$W = \frac{2 \cdot \pi}{\Delta} (R_1^2 - (R_1 - \delta)^2) \quad (5.4)$$

In the case described each unit length is divided into small units around the circumference. In other words W can be integrated around the tether considering the circumference consists of infinitesimally small linear increments. In order to do this one must know the nominal radius of the tether, which is known to be $r_{tether} = 18.7mm$. The integration is done over the circumference for small increments of length dL_{tether} . These increments can be calculated using the radius and the fact that for small angles $\sin \theta \approx \theta$.

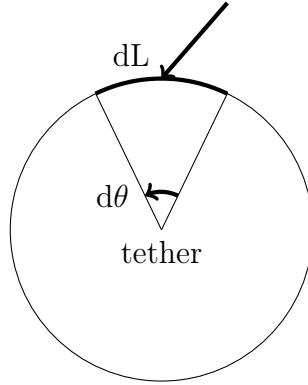


Figure 5.8: Visualization of integration

$$dL_{tether} = r_{tether} \cdot d\theta$$

This can be integrated for all valid angles, and in this case the entire circumference. L_{tether} can therefore be described by the following.

$$L_{tether} = \int_0^{2\pi} r_{tether} \cdot d\theta = r_{tether} \cdot 2\pi$$

The contact force of the tether and the two wheels, also considered the normal force between them, can then be calculated.

$$N = W \cdot L_{tether} = \frac{r_{tether} \cdot 4 \cdot \pi^2}{\Delta} (R_1^2 - (R_1 - \delta)^2) \quad (5.5)$$

If one considers the earlier example, where the maximum stress was set to 20MPa and the corresponding deformation of the TPR rubber was 2.77mm, one could then proceed to calculate the normal force this would induce between the tether and the wheels.

$$N = \frac{18.7 \cdot 4 \cdot \pi^2}{84.15} (230^2 - (230 - 2.77)^2) = 11111N \approx 11.1kN$$

The main motivation for finding the normal force, would be to calculate what the minimum friction coefficient between the materials in contact would need to be at different stresses. The maximum amount of force the tension wheel could transfer into pulling force on the tether is described by the following simple relation.

$$R = N \cdot \mu$$

IKM has provided information that the largest pulling force that is needed to operate the TMS is a pulling force of approximately $R \approx 3kN$. The minimum value of friction coefficient when the contact pressure on the tether is 20 MPa can then be calculated.

$$\mu_{min} = \frac{R}{N} = \frac{3kN}{11.1kN} \approx 0.27$$

In order to get a better understanding of how the necessary friction coefficient is calculated, one can study the graph below. For all different values of indentation one can see the necessary minimum friction coefficient to operate the TMS. The data is based on the nominal tether diameter of 37.4mm and the nominal thickness of the outer rubber layer being the nominal 3.5mm.

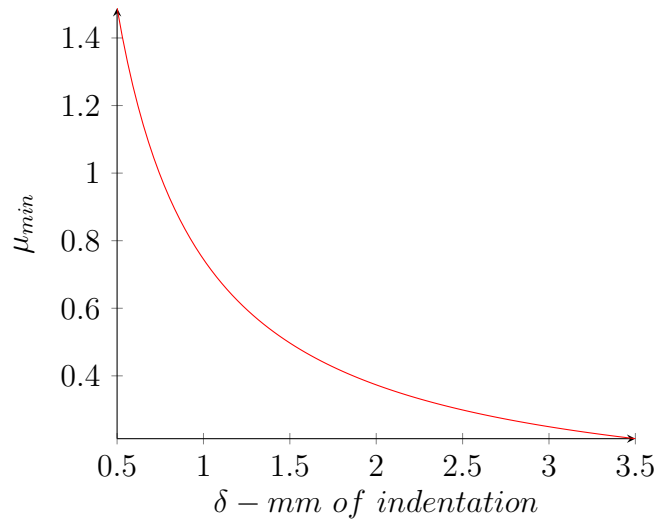


Figure 5.9: Friction coefficient per indentation at nominal tether diameter

Consideration of uncertain tether diameter

There are both pros and cons with operating the TMS using squeezing. The normal force increase allows for less attention being spent on finding materials with extreme friction coefficients. The squeezing does however provide issues, as there may be a fine line between squeezing sufficiently and squeezing too much. The tethers diameter is said to be 37.4mm, but there are some uncertainties with this number, as the cables diameter is measured with an uncertainty of 1mm according to Nexans. Considering a 1mm thicker or thinner tether changes the calculations to some extent. If the tether is 1mm thicker, the squeezing will increase by 0.5 mm around the circumference. Equally if the tether is 1mm thinner, the squeezing will decrease around the circumference. The result may then be that there is not enough squeeze to be able to transfer the normal force necessary, and therefore this may induce slipping. Slipping is considered to cause extensive wear on the tether and tension wheel, and is something that should be avoided. It is therefore necessary to calculate how much squeezing would occur in the range of 1mm thicker or thinner tether, and how that affects the load on the cable and also necessary friction coefficients.

The following calculations will be strongly dependent on an accurate measurement of the compressive modulus of the TPR rubber, which is previously estimated to be 4.1 MPa. In a situation where the compressive modulus is

higher, the material would be stiffer, and the normal force would be larger for each given indentation. In an opposite situation where the modulus of compression is lower, the material would be softer, and one would end up with a lower normal force between the tether and tension wheel. It is therefore in IKM's interest to experimentally find the most accurate value of this parameter, so that one can find out how the squeezing procedure can best be optimized.

If one assumes that most of the diameter uncertainty is due to different thickness of the outermost layer, the TPR layer, one will be able to calculate what forces is acting on the tether at the different squeezing limits. As the tethers diameter is 37.4mm and there is an uncertainty of 1mm, the tethers diameter at its thickest will be 2mm larger then the diameter at its thinnest. Considering the thickest and thinnest tether possible, the thickness of the outer TPR layer at all points will be in the interval [3mm, 4mm]. The variation in thickness may be handled by compressing the maximum thickness with an amount the tether will be able to handle, and then calculating how much compression this measurement would give the cable at its thinnest. E.g. if the 4mm TPR layer is allowed to compress 30% this means that the total compression is about 1.33mm. When the tether moves along and an area where the tether is thinner comes by, the TPR layer may now only be 3mm thick. As the 4mm layer was compressed 1.33mm, the thinner 3mm layer will be compressed only about 0.33mm or 11%. To figure out if this is sufficient, one must then calculate the normal force this maximum compression of 11% provides, and if it is sufficient to operate the TMS. The key to optimizing this problem would be to find a limit of which the squeezing of the 4mm layer is at its maximum, and then hopefully achieve a normal force value for the 3mm layer that is acceptable. A value for the compressive yield strength of copper was previously found to be 45 MPa, which means that the contact pressure must never exceed this value. With these considerations in mind one can look to equation 5.3 to calculate what stress the deformation will cause at different TPR layer thickness. The equations variables are given at $R_1 = 230mm, t \in [3mm, 4mm]$ and δ being the indentation in mm.

For calculations sake one would want to see how much stress is related to some given deformation of the thickest layer, and what normal force this would correspond to in the thinnest layer. This is because the limiting factor for the thickest rubber layer is exceeding allowable stress, and for the thinnest layer the limiting factor is the necessary friction coefficient. The calculations must therefore reflect a solution where the maximum stress is as low as possible, while keeping the minimum friction coefficient at an achiev-

able value. The deformation levels of the thickest TPR layer (t=4mm) used in the calculation are set to the following values, and the corresponding stress is also listed.

- $\delta_1 = 3mm \longrightarrow \sigma_1 \approx 14.75MPa$
- $\delta_2 = 2.5mm \longrightarrow \sigma_2 \approx 6.22MPa$
- $\delta_3 = 2mm \longrightarrow \sigma_3 \approx 3.24MPa$
- $\delta_4 = 1.5mm \longrightarrow \sigma_4 \approx 1.83MPa$

Now that the stress values are identified, one could go about calculating the normal force these different indentation depths induce at the thinnest rubber layer. Each of the indentation depths at the thickest layer is, as previously explained, 1mm deeper than the indentation depths at the thinnest level (t=3mm). This means that $\delta_{n,new} = \delta_n - 1$. Using the new indentation depths in equation 5.5 with the other parameters being kept constant, one ends up with the following corresponding normal-forces and minimum value of friction coefficients.

- $\delta_1 = 3mm \longrightarrow \delta_{1,new} = 2mm \longrightarrow N_1 \approx 8kN \longrightarrow \mu_1 = 0.375$
- $\delta_2 = 2.5mm \longrightarrow \delta_{2,new} = 1.5mm \longrightarrow N_2 \approx 6kN \longrightarrow \mu_2 = 0.5$
- $\delta_3 = 2mm \longrightarrow \delta_{3,new} = 1mm \longrightarrow N_3 \approx 4kN \longrightarrow \mu_3 = 0.75$
- $\delta_4 = 1.5mm \longrightarrow \delta_{4,new} = 0.5mm \longrightarrow N_4 \approx 2kN \longrightarrow \mu_4 = 1.5$

The results show some minimum friction coefficients as well as some maximum stresses at different indentation levels of the thickest tether diameter. The values indicates that to operate the TMS safely one would need to operate in an interval that does not allow large stress concentration to form, as well as having an acceptable minimum friction coefficient value. For instance one could say that if 0.5 friction coefficient is easily achieved, then squeezing more than 2.5mm at the thickest tether diameter and thus 1.5mm at the thinnest tether diameter is unnecessary. For nominal tether diameter this would correspond to 2mm of indentation.

Final thoughts on the squeezing model

One could do multiple steps to improve the accuracy of the calculations done in the analysis of the squeezing effects. The most important steps one could do is likely one or more of the following.

- Find the exact compressive modulus of the TPR rubber
- Minimize tether diameter uncertainty
- Find out what deformation can be expected from the other elements in contact. E.g. the core as well as the tension wheel
- Experimentally model the TPR materials specific stress intensification factor

Although the values used in the calculations do seem to add up to a certain extent, there is still room for significant improvement of the calculated result. For instance, the values found in the analysis says squeezing the tether at nominal diameter by 2.77mm around the circumference would cause internal stress of 20MPa. However, IKM data suggest that z-kinks was formed while squeezing about 1.85mm at 4 points (2 v-shaped grooves). The uncertain tether diameter tells us that the maximum indentation IKM has experienced would be $\delta = 1.85mm + 0.5mm \approx 2.35mm$. In other words, the model created allow more compression of the entire tether circumference than IKM has experienced when compressing only some parts of the circumference. The reason for this discrepancy is believed to be mainly due to the factors of inaccuracy listed above. The first and last point listed are likely the biggest contributor of inaccuracy in the results. As mentioned in the theory, the stress intensification factor used is made especially for a certain type of rubber material. This means that the factor is most likely somewhat different for the specific rubber material used in the tether in question. The compressive modulus used in the calculations is also an estimate as data from Nexans, the tether producer, only includes the tensile modulus. In order to find the values of interest, one would need to do some material testing of the TPR rubber. The simplest way to do this and get valuable results, would be to create a compressive stress - strain curve for the relevant stress interval. This way one could calculate how much strain the material would experience under the given load, and by that a maximum allowed indentation. The experimental values could then be used directly when designing the TMS, and one could simply avoid having to calculate the squeezing limit mathematically.

To further optimize the model, one would need to find out how much the other elements of the tether as well as the tension wheel will deform during operation. This will increase the amount of deformation possible, but it is unknown to what extent. The other elements in the cable is likely the most negligible factor, as the core consist of conductors, some protective PE layers and aramid armouring yarn. The core and armouring yarn will not likely deform much, and the PE layers are quite a lot thinner than the outer TPR layer. The tension wheel consist of rubber and metal, and how much deformation is possible will be dependant on how much of the cross section is rubber, and also the geometry of the metal-rubber boundary.

If one were to choose a tether where the protective outer sheet is thicker, one could squeeze the cable more while still being able to operate below stress limits. As the stress corresponds to strain, a thicker protective rubber layer would allow extra millimeters of indentation, which again would make the interval between sufficient and too much strain larger. If the safe squeeze interval is larger, it is easier for IKM to ensure that operation is done safely.

5.3 Material suggestions

The material suggestion of the tension wheel have a very important role when it comes to the friction as well as the wear and lifespan. These two factors often form a contradiction. On one hand, a lot of friction is wanted to avoid slips. On the other hand, high wear resistance is wanted for long lasting lifespan of materials.

5.3.1 Wear

Since there are a lot of different rubber mixtures and the wear properties of rubber itself is highly versatile and dependent on many different factors, it is difficult to come up with specific results that points to one material that sticks out from the rest. Instead, the approach is to compare several rubber compounds, in regards to the factors that most likely will have an impact. The main factors in this situation are compact set, creep, abrasion resistance, adhesion, tear resistance, water swell resistant and solvent resistance against water. The most important factors perhaps being abrasion resistance and adhesion when it comes to the lifespan, and that the material thrives in the ocean environment. An unwanted quality is swelling of the rubber submerged under high pressures. In figure 5.11 different rubber compounds are listed up, comparing them to each other using a grading system from A(excellent) to NR(Not recommended). The table in figure 5.13 similarly list up rubber compounds which are rated between Green(Very good) and White(Not recommended). In figure 5.14 the rubber compounds are rated between Excellent and Poor.

TABLE 33.1 Designation and Composition of Common Elastomers

ASTM designation	Common name	Chemical composition
NR	Natural rubber	<i>cis</i> -Polyisoprene
IR	Synthetic rubber	<i>cis</i> -Polyisoprene
BR	Butadiene rubber	<i>cis</i> -Polybutadiene
SBR	SBR	Poly (butadiene-styrene)
IIR	Butyl rubber	Poly (isobutylene-isoprene)
CIIR	Chlorobutyl rubber	Chlorinated poly (isobutylene-isoprene)
BIIR	Bromobutyl rubber	Brominated poly (isobutylene-isoprene)
EPM	EP rubber	Poly (ethylene-propylene)
EPDM	EPDM rubber	Poly (ethylene-propylene-diene)
CSM	Hypalon	Chloro-sulfonyl-polyethylene
CR	Neoprene	Poly chloroprene
NBR	Nitrile rubber	Poly (butadiene-acrylonitrile)
HNBR	Hydrogenated nitrile rubber	Hydrogenated poly (butadiene-acrylonitrile)
ACM	Polyacrylate	Poly ethylacrylate
ANM	Polyacrylate	Poly (ethylacrylate-acrylonitrile)
T	Polysulfide	Polysulfides
FKM	Fluoroelastomer	Poly fluoro compounds
FVMQ	Fluorosilicone	Fluoro-vinyl polysiloxane
MQ	Silicone rubber	Poly (dimethylsiloxane)
VMQ	Silicone rubber	Poly (methylphenyl-siloxane)
PMQ	Silicone rubber	Poly (oxydimethyl silylene)
PVMQ	Silicone rubber	Poly (polyoxymethylphenyl-silylene)
AU	Urethane	Polyester urethane
EU	Urethane	Polyether urethane
GPO	Polyether	Poly (propylene oxide-allyl glycidyl ether)
CO	Epichlorohydrin homopolymer	Polyepichlorohydrin
ECO	Epichlorohydrin copolymer	Poly (epichlorohydrin-ethylene oxide)

Figure 5.10: Overview of the different rubber materials that are compared in figure 5.11 [8].

TABLE 33.2 Relative Properties of Various Elastomers

ASTM designation	NR		BR		SBR		IIR		EPM		CSM		CR		NBR		HNBR		ACM		T		FKM		FVMQ		PMQ,		VMO		AU		GPO		CO		ECO	
	30-90	40-90	40-80	3000	3500	600	850	3000	40-90	45-100	4000	4000	30-95	40-95	40-90	40-85	60-90	40-80	30-90	35-100	40-90	40-85	1500	3000	40-80	40-80	30-90	35-100	40-90	40-90	3000	2500						
Durometer range	4500	3000	3500	3000	3500	600	850	3000	40-90	45-100	4000	4000	40-95	40-90	40-85	60-90	40-80	40-80	30-90	35-100	40-90	40-85	1500	3000	40-80	40-80	30-90	35-100	40-90	40-90	3000	2500						
Tensile max, psi	650	650	600	850	600	600	600	600	500	500	600	600	4000	4000	4000	4000	4000	4000	4000	4500	2500	4500	2500	4500	2500	4500	2500	4500	2500	4500	2500	4500	2500					
Elongation max., %	A	B	B	B	B	B	B	B	B	B	B	B	B	B	B	B	B	B	B	B	B	B	B	B	B	B	B	B	B	B	B	B	B					
Compression set	A	B	B	B	B	B	B	B	B	B	B	B	B	B	B	B	B	B	B	B	B	B	B	B	B	B	B	B	B	B	B	B	B					
Creep	A	B	B	B	B	B	B	B	B	B	B	B	B	B	B	B	B	B	B	B	B	B	B	B	B	B	B	B	B	B	B	B	B					
Resilience	High	High	Med.	Low	Med.	Low	Med.	Low	Med.	Low	Med.	Low	Med.	Low	Med.	Low	Med.	Low	Med.	Low	Med.	Low	Med.	Low	Med.	Low	Med.	Low	Med.	Low	Med.	Low	Med.	Low				
Abrasion resistance	A	A	A	C	B	A	C	B	A	A	A	A	A	A	A	A	A	A	A	A	A	A	A	A	A	A	A	A	A	A	A	A	A	A				
Tear resistance	A	B	C	B	C	B	A	B	C	B	B	B	B	B	B	B	B	B	B	B	B	B	B	B	B	B	B	B	B	B	B	B	B	B				
Heat aging at 212°F	C-B	C	B	A	B-A	B-A	B-A	B-A	B-A	B-A	B-A	B-A	B-A	B-A	B-A	B-A	B-A	B-A	B-A	B-A	B-A	B-A	B-A	B-A	B-A	B-A	B-A	B-A	B-A	B-A	B-A	B-A	B-A	B-A	B-A			
$T_g, ^\circ\text{C}$	-73	-102	-62	-73	-65	-17	-43	-26	-32	-24,-54	-59	-23	-69	-127,-86	-23,-34	-67	-25,-46	-23,-34	-67	-25,-46	-23,-34	-67	-25,-46	-23,-34	-67	-25,-46	-23,-34	-67	-25,-46	-23,-34	-67	-25,-46	-23,-34	-67	-25,-46			
Weather resistance	D-B	D	D	A	A	A	A	A	A	A	A	A	A	A	A	A	A	A	A	A	A	A	A	A	A	A	A	A	A	A	A	A	A	A	A			
Oxidation resistance	B	B	C	A	A	A	A	A	A	A	A	A	A	A	A	A	A	A	A	A	A	A	A	A	A	A	A	A	A	A	A	A	A	A	A			
Ozone resistance	NR-C	NR	NR	NR	NR	NR	NR	NR	NR	NR	NR	NR	NR	NR	NR	NR	NR	NR	NR	NR	NR	NR	NR	NR	NR	NR	NR	NR	NR	NR	NR	NR	NR	NR	NR			
Solvent resistance																																						
Water	A	A	B-A	A	A	B	B	B	B	B	B	B	B	B	B	B	B	B	B	B	B	B	B	B	B	B	B	B	B	B	B	B	B	B	B			
Ketones	B	B	B	A	B-A	B	C	D	D	D	D	D	D	D	D	D	D	D	D	D	D	D	D	D	D	D	D	D	D	D	D	D	D	D	D			
Chlorohydrocarbons	NR	NR	NR	NR	NR	NR	NR	NR	NR	NR	NR	NR	NR	NR	NR	NR	NR	NR	NR	NR	NR	NR	NR	NR	NR	NR	NR	NR	NR	NR	NR	NR	NR	NR	NR	NR		
Kerosene	NR	NR	NR	NR	NR	NR	NR	NR	NR	NR	NR	NR	NR	NR	NR	NR	NR	NR	NR	NR	NR	NR	NR	NR	NR	NR	NR	NR	NR	NR	NR	NR	NR	NR	NR	NR		
Benzol	NR	NR	NR	NR	NR	NR	NR	NR	NR	NR	NR	NR	NR	NR	NR	NR	NR	NR	NR	NR	NR	NR	NR	NR	NR	NR	NR	NR	NR	NR	NR	NR	NR	NR	NR	NR		
Alcohols	B-A	B	B	B	B	B	B	B	B	B	B	B	B	B	B	B	B	B	B	B	B	B	B	B	B	B	B	B	B	B	B	B	B	B	B			
Water glycol	B-A	B-A	B	B	B	B	B	B	B	B	B	B	B	B	B	B	B	B	B	B	B	B	B	B	B	B	B	B	B	B	B	B	B	B	B			
Lubricating oils	NR	NR	NR	NR	NR	NR	NR	NR	NR	NR	NR	NR	NR	NR	NR	NR	NR	NR	NR	NR	NR	NR	NR	NR	NR	NR	NR	NR	NR	NR	NR	NR	NR	NR	NR	NR		

A = excellent, B = good, C = fair, D = use with caution, NR = not recommended
SOURCE: *Seals Eastern, Inc.*

33.6

Figure 5.11: This table shows comparisons of different rubber mixtures.[8]

ELASTOMER RUBBER COMPOUNDS TYPES AND REFERENCES						
General Description	Chemical Description	Abbreviation (ASTM 1418)	ISO/DIN 1629	Other Trade names & Abbreviations	ASTM D2000 Designations	
<u>Nitrile</u>	Acrylonitrile-butadiene rubber	NBR	NBR	Buna-N	BF, BG, BK, CH	
<u>Hydrogenated Nitrile</u>	Hydrogenated Acrylonitrile-butadiene rubber	HNBR	(HNBR)	HNBR	DH	
<u>Ethylene-Propylene</u>	Ethylene propylene diene rubber	EPDM	EPDM	EP, EPT, EPR	BA, CA, DA	
<u>Fluorocarbon</u>	Fluorocarbon Rubber	FKM	FPM	Viton®, Fluorel®	HK	
<u>Chloroprene</u>	Chloroprene rubber	CR	CR	Neoprene	BC, BE	
<u>Silicone</u>	Silicone rubber	VMQ	VMQ	PVMQ	FC, FE, GE	
<u>Fluorosilicone</u>	Fluorosilicone rubber	FVMQ	FVMQ	FVMQ	FK	
<u>Polyacrylate</u>	Polyacrylate rubber	ACM	ACM	ACM	EH	
<u>Ethylene Acrylic</u>	Ethylene Acrylic rubber	AEM	AEM	Vamac®	EE, EF, EG, EA	
<u>Styrene-butadiene</u>	Styrene-butadiene rubber	SBR	SBR	SBR	AA, BA	
<u>Polyurethane</u>	Polyester urethane / Polyether urethane	AU / EU	AU / EU	AU / EU	BG	
<u>Natural rubber</u>	Natural rubber	NR	NR	NR	AA	

Figure 5.12: List of rubbers to comparison in figure below.[9]

	Very Good	Good	Average	Poor	Not Recommended							
Basic Property	NBR	HNBR	EPDM	FKM	CR	ACM	AEM	SBR	AU/EU	VMQ	FVMQ	NR
Economy of Material	●	●	●	●	●	●	●	●	●	●	●	●
Compression Set Resistance	●	●	●	●	●	●	●	●	●	●	●	●
Resilience (Rebound)	●	●	●	●	●	●	●	●	●	●	●	●
Tear Strength	●	●	●	●	●	●	●	●	●	●	●	●
Heat Aging Resistance	●	●	●	●	●	●	●	●	●	●	●	●
Ozone Resistance	●	●	●	●	●	●	●	●	●	●	●	●
Resistance to Oil & Grease	●	●	●	●	●	●	●	●	●	●	●	●
Fuel Resistance	●	●	●	●	●	●	●	●	●	●	●	●
Water Swell Resistance	●	●	●	●	●	●	●	●	●	●	●	●
Gas Impermeability	●	●	●	●	●	●	●	●	●	●	●	●
Dynamic Service / Abrasion Res.	●	●	●	●	●	●	●	●	●	●	●	●
High Temperature - Standard	212 °F	300 °F	300 °F	390 °F	250 °F	300 °F	300 °F	212 °F	175 °F	450 °F	400 °F	220 °F
High Temperature - Special	250 °F	-	-	-	-	-	-	-	-	480 °F	-	-
Low Temperature - Standard	-22 °F	-22 °F	-60 °F	5 °F	-40 °F	-60 °F	-40 °F	-50 °F	-60 °F	-75 °F	-75 °F	-60 °F
Low Temperature - Special	-60 °F	-40 °F	-	-30 °F	-	-	-	-	-	-	-	-

Figure 5.13: Abilities of different rubber compounds rated from very good to not recommended.[9]

Elastomer	Abrasion Resistance
Nitrile	Excellent
Polyurethane	Excellent
SBR	Excellent
Thermoplastic Elastomer	Good / Excellent
Natural Rubber	Good / Excellent
Butyl	Good
Hypalon	Good
Neoprene	Good
Vamac	Good
Viton	Good
EPDM	Fair
Silicone	Fair

Figure 5.14: Different rubber compounds ability to abrasion resistance rated from poor to excellent.[26]

Looking at figure 5.11, it is the rubber mixtures NR (Natural rubber), HNBR (Hydrogenated nitrile rubber), NBR (Nitrile rubber), BR (Butadiene rubber), FKM (Fluoroelastomer) and CR (Neoprene) that stands out positively, scoring highly in the desired qualities.

From figure 5.13, the rubber mixtures of nitrile, polyurethane, SBR, thermoplastic elastomer and natural rubber show the most promising qualities.

In figure 5.14, the rubber mixtures NR, HNBR, EPDM, NBR, SBR and AEM show the best results for the wanted attributes.

Since there is somewhat of a danger of the TMS being exposed to oils, the rubber mixtures EPDM, AEM, SBR, NR, BR and CR are taken out of consideration. Comparing the different tables, one ends up the following

rubber mixtures which are considered most suitable:

- HNBR
- NBR

HNBR and NBR have a lot of similar qualities, but NBR is a lot cheaper. With this in mind, the focus is directed to NBR for the rest of the chapter. The wear properties for every rubber mixture can be customized by using additives.[9] To get a better understanding of the wear of NBR, one can look to the studies done by Nong Tian, Tingmei Wang, Kun Wang and Qunji Xue called "Friction and wear properties of NBR/PVC composites".[16] The studies describe the wear and friction attributes of NBR with different levels of PVC composites. The hardness of the NBR was initially around 68 Shore A. As the PVC content was increased, the hardness was also increased.

The wear rate is an important parameter describing the wear of the material. The wear rate in this study was calculated by taking mass loss divided by the sliding distance

$$W = \frac{m_1 - m_0}{L} \quad (5.6)$$

where W is the wear rate, m_1 is the initial weight, m_0 is the weight after testing and L is the sliding distance. The results for the different levels of PVC content in NBR is shown in figure 5.15.

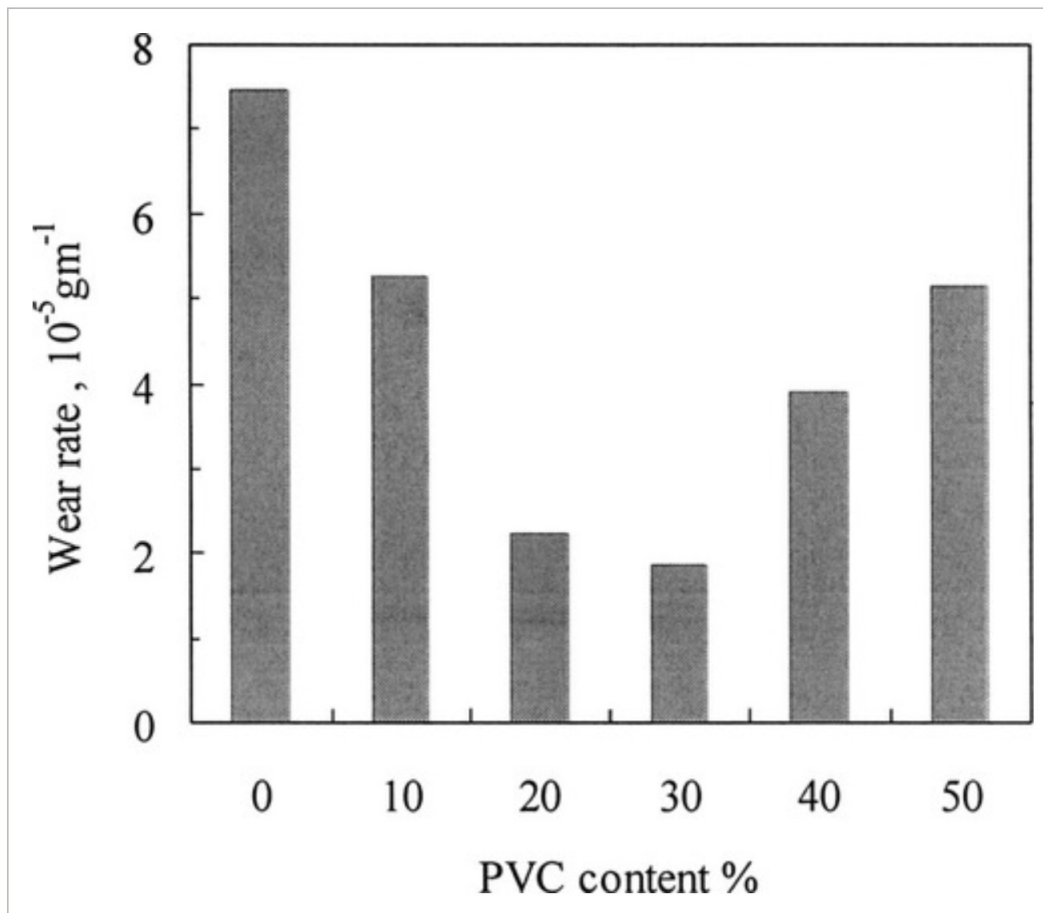


Figure 5.15: Wear rate with respect to PVC content. [16]

The test suggests that the wear is the least when the PVC content is at 30%. At 0% PVC content the wear rate is approximately $7.5 \cdot 10^{-5} \text{ g/m}$. At 30% it is around $2 \cdot 10^{-5} \text{ g/m}$. This means a reduction at 70-75%. It also suggests that the wear rate is not only dependent hardness of the material, as the wear rate increases again after the PVC content exceeds 30%. The maximum wear happens when it is 0% PVC, in other words, pure NBR.

Rubber can at certain pressures swell up. The engineers at IKM has informed that this affects both the tribological and mechanical properties, and thus this kind of swelling is unwanted. A study of how carbon black additive affect the swelling of NBR and SBR called "Effect of carbon black loading on the swelling and compression set behavior of SBR and NBR rubber compounds"[23], can provide further information about this topic. One of the

experiments done in this study was measuring the swelling ratio compared to the exposure time at different temperatures. It is unclear what exact temperature the tension wheel might be during activity, and how much heat is generated by friction. To get a better understanding of the swelling, two tests from the study is included. The tests show a variety of temperatures including $T = 25^{\circ}\text{C}$ and $T = 70^{\circ}\text{C}$. The swelling ratio was defined as

$$Q\% = \frac{M_t - M_0}{M_0} \cdot 100 \quad (5.7)$$

where M_0 where the mass of the test piece before the test and M_t was the mass after the test. The test resulted in the graphs shown in figure 5.16 and 5.17

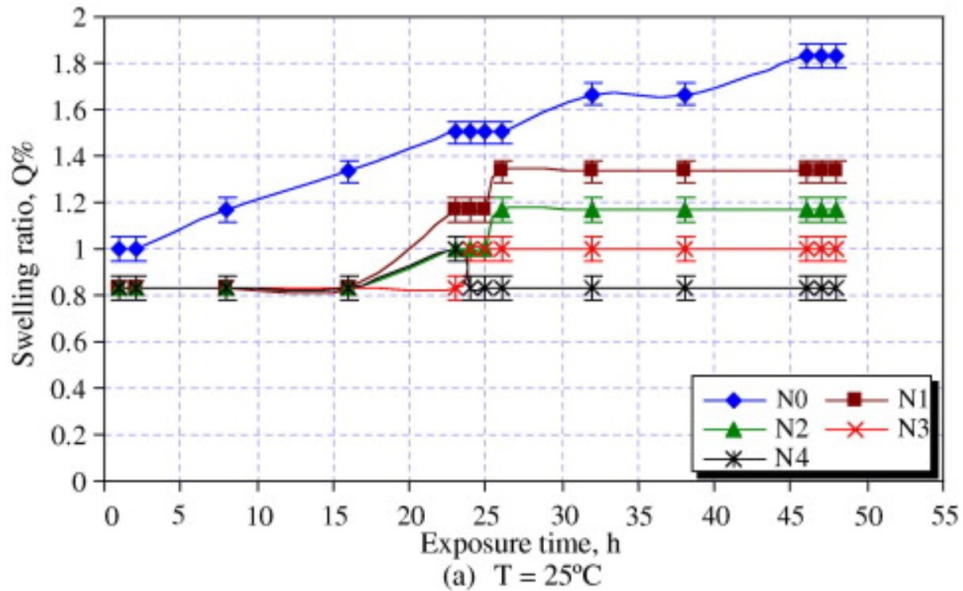


Figure 5.16: Swelling of NBR containing carbon black in 25°C [23].

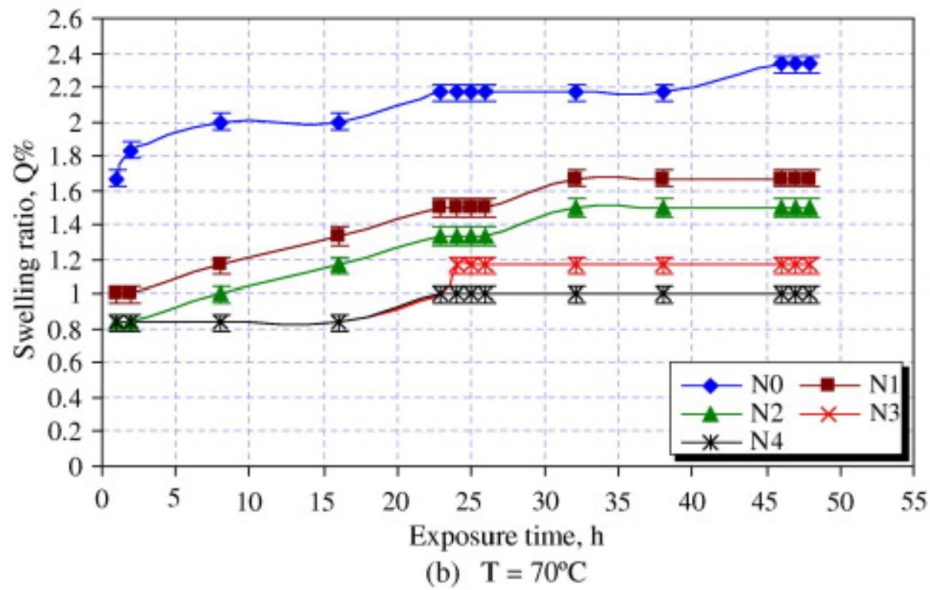


Figure 5.17: Swelling of NBR containing carbon black in 70°C [23]

The difference between N0, N1, N2, N3 and N4 are the levels of carbon black contained in the NBR, with N0 containing no carbon black and N4 containing the most carbon black. Seen from the graphs the compound least affected by swelling is the test pieces with most carbon black content. At temperatures of 25°C, one can observe that the swelling of the test pieces containing some amount of carbon black is kept constant up to about 15 hours, before the different compounds' swelling behaviour varies.

5.3.2 Friction

Frictional properties of the material might be the most important parameter related to the tension wheel of the TMS. As mentioned in the theory, the frictional properties are dependent on many different factors. One important factor is the adhesive strength. As the frictional properties of the material are very complex and relies on a lot of information, the same approach for the wear of the material is used in the aspect of friction as well. The main point of reference to achieve optimal frictional properties is the adhesive strength of the material. The following figure, like the figures in chapter 5.3.1, contains a comparison of the various properties of different rubber materials, including adhesion.

ANSI/ASTM Designation	NR/IR	AU/EU	CR	EPDM	FKM	HNBR	NBR	TFE/P	VMQ
Common Name	Natural Rubber	Polyurethane	Chloroprene (Neoprene)	EPDM	Viton®	Hydrogenated Nitrile	Nitrile	Aflas®	Silicone
Low Temp	-60°F	-40°F	-30°F	-40°F	-10°F	-22°F	-30°F	25°F	-80°F
High Temp	220°F	175°F	212°F	300°F	400°F	300°F	250°F	450°F	420°F
Durometer Shore A	30-90 Shore A	10-100 Shore A	15-95 Shore A	30-90 Shore A	50-95 Shore A	55-95 Shore A	20-100 Shore A	60-100 Shore A	25-85 Shore A
Abrasion	Fair - Good	Excellent - Outstanding	Very Good - Excellent	Good - Excellent	Good	Good-Excellent	Good-Excellent	Good-Excellent	Poor
Adhesion	Excellent	Excellent	Excellent	Good - Excellent	Fair - Good	Excellent	Excellent	Fair - Good	Excellent
General Properties	Excellent physical properties including abrasion and low temperature resistance. Poor resistance to petroleum-based fluids.	Good aging and excellent abrasion, tear, and solvent resistance. Poor high temperature properties.	Good Weathering Resistance. Flame retarding. Moderate resistance to petroleum-based fluids.	Excellent ozone, chemical, and aging resistance. Poor resistance to petroleum-based fluids.	Excellent oil and air resistance both at low and high temperatures. Very good chemical resistance.	Excellent heat and oil resistance, improved fuel and ozone resistance (approximately 5X) over Nitrile Good abrasion resistance. Decreased elasticity at low temperatures with hydrogenation over standard nitrile.	Excellent resistance to petroleum-based fluids. Good physical properties.	High temperature polymer, good overall chemical resistance, poor compression set and a high minimum working temperature.	Excellent high and low temperature properties. Fair physical properties.
General Chemical Resistance									
Resistant to:	Most moderate chemicals, wet or dry, organic acids, alcohols, ketones, aldehydes.	Ozone, hydrocarbons, moderate chemicals, fats, oils, greases.	Moderate chemicals and acids, ozone, oils, fats, greases, many oils, and solvents.	Animal and vegetable oils, ozone, strong and oxidizing chemicals.	All aliphatic, aromatic and halogenated hydrocarbons, acids, animal and vegetable oils.	Many hydrocarbons, transmission fluids, refrigerants, diluted acids, hydraulic fluids, silicone oils, vegetable and animal fats and oils, water and steam.	Many hydrocarbons, fats, oils, greases, hydraulic fluids, chemicals.	Highly resistant to a wide range of chemicals, such as acid, base and steam. Superior resistance to strong bases in comparison with FKM.	Moderate or oxidizing chemicals, ozone, concentrated sodium hydroxide.
Attacked by:	Ozone, strong acids, fats, oils, greases, most hydrocarbons.	Concentrated acids, ketones, esters, chlorinated and nitro hydrocarbons.	Strong oxidizing acids, esters, ketones, chlorinated, aromatic and nitro hydrocarbons.	Mineral oils and solvents, aromatic hydrocarbons.	Ketones, low molecular weight esters and nitro containing compounds.	Chlorinated hydrocarbons, ketones, strong acids.	Ozone (except PVC blends), ketones, esters, aldehydes, chlorinated and nitro hydrocarbons.	Attacked to varying degrees by strong caustics; polar solvents such as acetone and MEK; ammonia; hydrogen sulfide; high pH amine corrosion inhibitors and red fuming nitric acid	Many solvents, oils, concentrated acids, dilute sodium hydroxide

Figure 5.18: Comparison of different elastomers.[17]

Figure 5.18 shows that the best materials with respect to adhesive forces are NR/IR (natural rubber), AU/EU (polyurethane), CR (neoprene), HNBR (hydrogenated nitrile), NBR (Nitrile) and VMQ (silicone). From figure 5.18, NBR show excellent adhesive properties making it suitable for high friction needs. From chapter 5.3.1 the NBR was assumed to be the most durable rubber compound and will be assumed to be the best fit regarding frictional

properties correspondingly.

Using knowledge from the study "Friction and wear properties of NBR/PVC composites", where friction and wear of NBR with different levels of PVC content are compared, one can see how the friction coefficient varies over different PVC contents. The friction coefficient in this study is between a steel ball and a surface of NBR/PVC,[16] and was measured with respect to PVC content with results shown in figure 5.19.

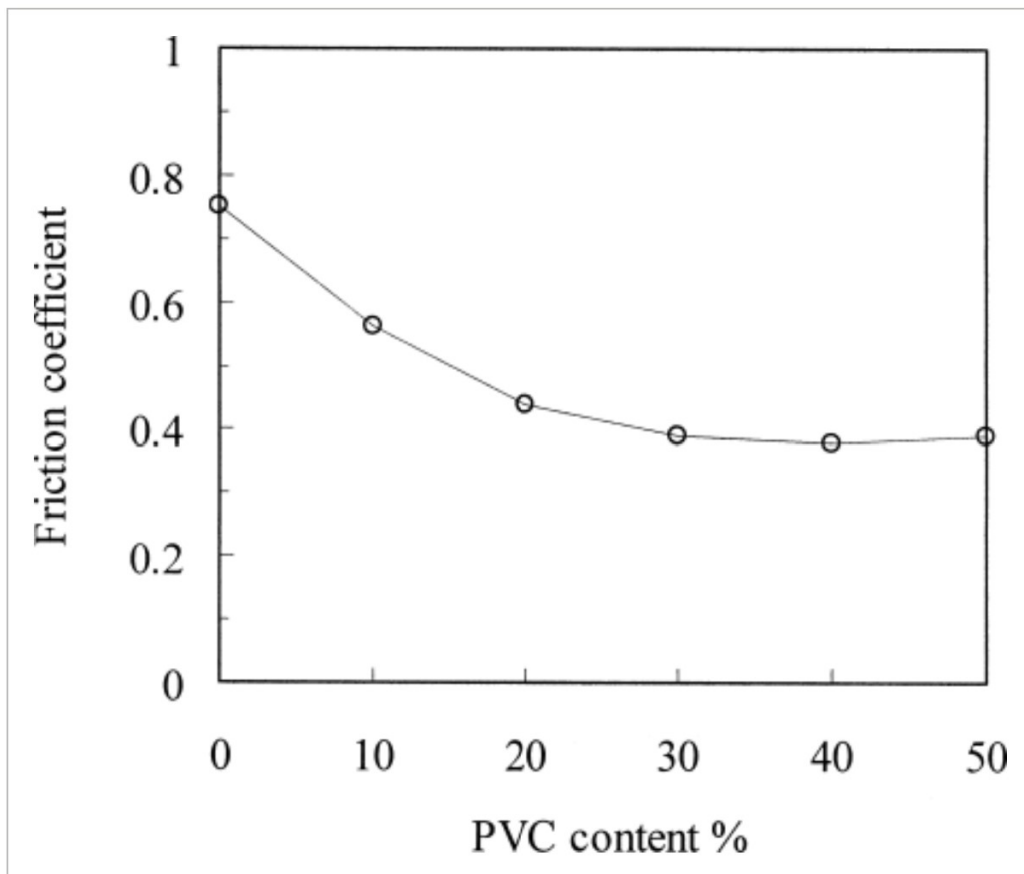


Figure 5.19: Friction coefficient as a function of PVC content.[16]

Seen in the figure above, the friction coefficient decreases as the PVC content increases. So for maximum friction coefficient, no PVC content is desired. The maximum coefficient of friction is roughly 0.75, and at 30-40% PVC content, about 0.4, which correlates to a 45-50% decrease.

5.3.3 Material choice with respect to friction and wear

Comparing the different tables, there is reason to believe that nitrile rubber (NBR) is a suitable rubber material for this particular task, as it has great tribological properties with respect to both friction and wear.

Friction and wear form a rivalry, as good frictional properties often increases wear, and good wear properties reduces friction. The task at hand is therefore to find the perfect balance of friction versus wear in the TMS. The perfect situation, theoretically, would be to have just enough friction force for the TMS to work perfectly to minimize the wear of the materials. The frictional properties is therefore considered the foundation for which materials to use.

How additives affect the tribological properties of nitrile rubber is clearly shown above. Content of PVC described how PVC affected the wear and frictional properties of NBR. The NBR/PVC compound showed a complex relation between the content of PVC and wear, as the content at which the wear was at minimum, was about 30%. The wear increased with more PVC content after the 30% mark. The frictional properties, similarly, decreased with more PVC content. The reduction of wear, from 0-30% PVC content, was 70-75% versus a 30-40% reduction of friction coefficient for the same PVC content interval. The question again is therefore; *what is the necessary friction coefficient between the tension wheel and tether?* This question is vital to answer to find the perfect content of the PVC content, if it was to be used.

Also from the analysis, was how carbon black (CB) affected the swelling of NBR. The results showed that swelling decreased for increasing content of CB, and therefore for the case of only minimizing swelling effect, should hold maximum carbon black content.

It would be very difficult to determine a specific rubber compound from only this information as it is unclear how PVC handle water, oils and high pressure, and similarly with carbon black. There probably are different additives that fulfills the same requirements at different, and maybe even better ways. There is limited information about these topics, and no studies have been found where relevant experiments have been conducted in similar environments as the TMS experiences. The engineers at IKM has observed that the friction coefficient decreases as the velocity between the surfaces increase. It is also observed that the friction coefficient is not necessarily constant for a given velocity. This suggests that the friction coefficient is dependent on whether the tension wheel has been accelerated or decelerated

to the velocity in question. This might have a correlation with the hysteresis of rubber. Since there is rolling contact between the surfaces, the amount of relative sliding between the tether and tension wheel is very much dependent on the slip ratio of the surfaces. Although this is known, how much it affects the friction is uncertain and the effect of velocity and slip ratio remains unclear. How the lubrication of sea water affects the same properties is also an unknown factor. Accordingly, there is not sufficient data to say anything specific about the actual friction and wear properties of the tension wheel and tether.

5.3.4 Method for when tension wheels should be replaced

This particular part of the thesis is highly dependent on several different factors. The tension wheel will not work flawlessly all the time and will eventually have slip ups where the friction force is not sufficient and the tether cable will slide along the tension wheel. These occurrences will happen unevenly, and it is hard to determine how much sliding is affecting the wear, considering there is not done any testing in this regard.

Since this is a theoretical thesis and there were lack of data from similar situations a proposed idea is to use wear indicators, often used on different parts on a motor vehicle, to determine when the tension wheel should be replaced. Treads wear indicators have an unknown effect on friction and wear. It would therefore be best to avoid any wear indicators such as these.

The proposed idea is to have two different colors for the rubber mixture, for example black and red, as modelled in figure 5.20. The red rubber mixture would be located at the base of the tension wheel and the black rubber mixture would be the surface. As the outer sheet of the black rubber mixture is being worn the closer it would get to the red rubber mixture. As soon as the user spots the red color at the tension wheel, it is time to replace it. This is a simple way about solving the problem, and easy for anyone to observe when to swap the worn tension wheel for a new one. The idea is that it would be better to involve indicators for when the wheel is too worn out, due to the unpredictability of the slip ups that IKM experience. The indicator is therefore a good mechanism for when the tension wheel should be replaced.

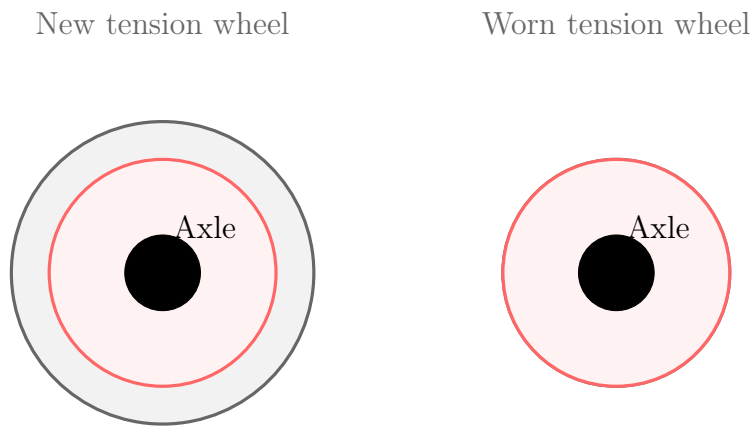


Figure 5.20: Idea for wear indicators on the tension wheel

There is an important correlation between the wear and squeezing effect. The squeezing effect is quite crucial for the TMS to get sufficient friction. Neglecting the possible polishing effects of wear, the indicators should be placed at the point of minimum squeeze required for the TMS to work properly. This is not necessarily the case. The use of wear indicators has no effect if it is not calculated how thick the black layer should be. Therefore, for the same reason as it is not possible to say anything about the number of rotations for when the tension wheel should be replaced, it has to be tested to determine the specific depth of the indicators.

5.4 Drum layout alterations

Even though the layout with the Lebus shell works remarkably on the M-TMS, IKM's desire in this regard is quite clear, that they want to alter it to a more economical favorable solution, namely a smooth drum solution. The smooth drum that IKM wants to apply to its M-TMS poses a series of problems that need resolving for it to be applied.

5.4.1 Smooth drum Lebus Shell layout

The question to be asked when considering a smooth drum for the M-TMS, is what tether pattern should be used. One could postulate that it is possible to lay the tether in a Lebus Shell like fashion, without the use of grooves. Since there are no grooves on the drum surface, it will be difficult for the tether to be able to follow a trajectory parallel to the flanges of the drum, and then only move across in the crossover sections like with the Lebus Shell configuration. To get such precise tether placement without the grooves, the tether would need to be in a extreme state of axial tension in addition to the spool guiding the tether would have to guide the tether with precision beyond what could be expected from it. Even if the tether theoretically could be laid on to the drum in such a Lebus-configuration without the grooves, there is no guarantee that the tether will lay itself in the manner that one would desire due to the extra uncertainties in spooling behaviour associated with the smooth drum (discussed in section 5.4.3).

5.4.2 Smooth drum helical layout

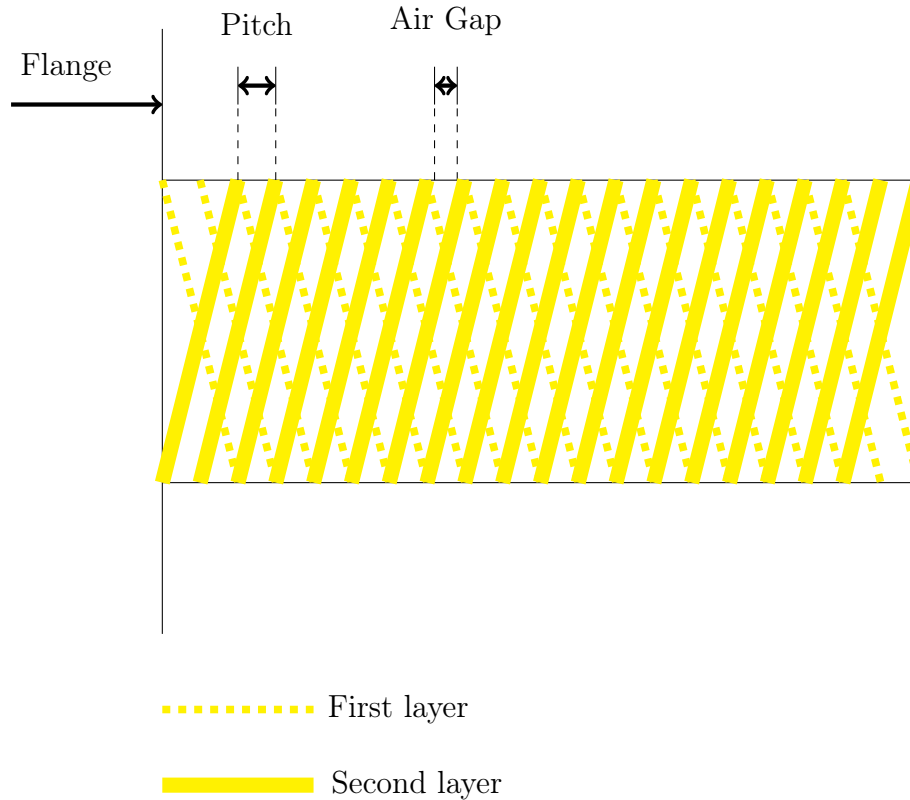


Figure 5.21: Simplified helical smooth drum layout.

Since it's unfeasible to have a Lebus Shell-like tether pattern on a smooth drum, some other pattern will need to be applied. The tether pattern will be of a helical fashion like shown in Figure 5.21. In this configuration, the tether gets placed in a helical fashion around the drum like a screw thread. After the spooling has gone all the way to the other flange, there would need to be an end filler to help get the tether onto the next layer. The next layer would lay itself in a helical fashion the other way, continuously crossing over the cables underneath while doing so. Theoretically in such a configuration the tether makes a perfect helix in each layer, providing the smooth spooling behavior desired for the M-TMS. Note that Figure 5.21 is not representative of the pitch one would need in a helical configuration, and just visualizes the pattern. The pitch would in a real world application be much smaller.

5.4.3 Helical layout complications

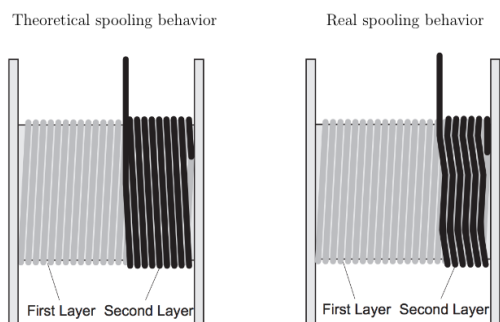


Figure 5.22: Smooth drum layout. [38]

Even though applying a smooth drum solution to the M-TMS in theory seems possible, research and testing indicates that it is not a straight forward task. The theoretical spooling behavior is as described in section 5.4.2, and is quite different from the actual spooling behavior, and it introduces some new problems. As seen in section 5.4.2, the tether will spool from one flange to another in the first layer in a helical fashion just like in the theoretical behavior. The rope will then lay itself on top of the previous layer and start to wrap the other way around the drum, and it is in these consecutive layers that the problems occurs. Here the tether will cross over the first wrap, before laying itself in between the wedge of two wraps. [38] This happens due to the axial tension in the cable combined with the rotary motion of the drum causing the force F described in Figure 5.23. When the tether moves over the first wrap, there must be a great enough static frictional force, f_s working between the tether to not make it slip in between the wedges. Since the static frictional force between the tether layers are not sufficient, the tether will start to slip, and lay itself in between the wedge. This is indicated by f_k in the second scenario in Figure 5.23, which is the scenario right before the tether is wedged. When wedged, the tether will follow the pattern of the wedge of the previous layer and therefore effectively spool in the wrong direction. Figure 5.22 shows the difference in spooling behavior from theoretical to real behavior. Note that the forces in all of the figures in this section are not to scale, and are drawn for conceptualizing purposes only.

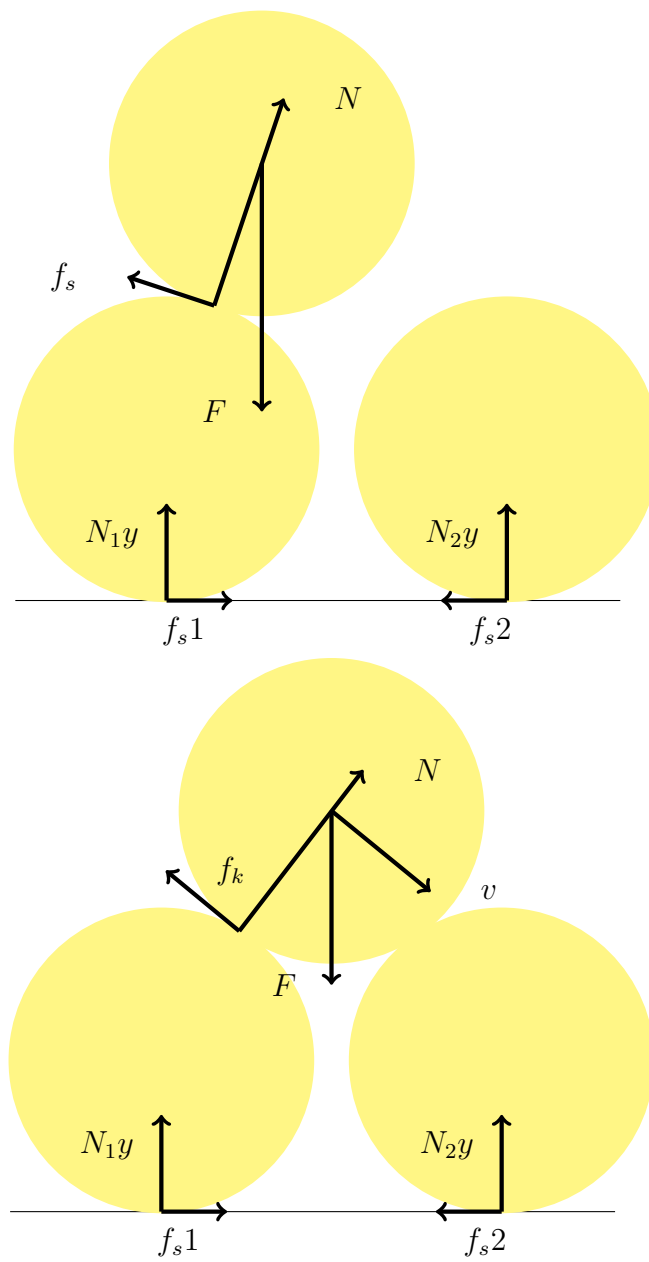


Figure 5.23: Simplified force scenario into a wedge in a helical layout

Consequences of real life smooth drum spooling behavior

What are the consequences of this real life spooling behavior on the smooth drum? Well first of all, it makes the spooling much more unpredictable. When the tether has gotten wedged as in the first scenario in Figure 5.24, the screw level winder moves in the opposite direction (to the left) of the wedge pattern of the first layer (to the right). The force scenario is visualized in Figure 5.24. There will then be a static friction force holding the tether from moving out of the wedge (indicated by f_s), while the screw level winder will provide more and more force (indicated by F_x) in the other direction. The tether from the previous revolution will also help push the tether to the side, and also contributes to the size of F_x . Since the cable is located in the wedge, it will not move out of it for a short period. As F_x grows, N will also get larger, and hence make f_s larger. When F_x is sufficient, the tether will start to slip, and the friction force will go from being static to kinetic. As mentioned in section 3.1.1, the coefficient of static friction is greater than the coefficient of kinetic friction, which means that the static friction force is also larger than the kinetic friction force. This shift in friction force leads to there suddenly being a net plus force in the horizontal direction. Also the normal force N will contribute less in the horizontal direction due to the tether sliding upwards, effectively making N tilt more vertically. The manner in which the tether goes over the wrap will be determined by the magnitude of the net force that is developed. With a large enough net force, the tether will slam over the next wrap in a forceful manner, causing complications. When the net force has made the tether go over another wrap, the tether will slam into the tether of the next wrap. Then the cycle starts all over again with the tether getting wedged, and moving in the tether pattern of the previous layer, and then powerfully slamming over yet another wrap. This vigorous behavior makes it difficult to prolong the service life of the tether. If slammed in to a wedge with too much force, there will be further complications when additional layers of tether are placed on the drum. The layer making the wedges will be crushed, and will also pinch the layer on top, potentially causing z-kinks in the part of the tether that gets wedged due to the potentially big contact pressures that could occur. If these consequences have major impact on the tethers lifespan would need to be tested before one could conclude anything, but there are serious implications with a smooth drum helical layout that would need to be addressed through testing before applying such layout to the M-TMS.

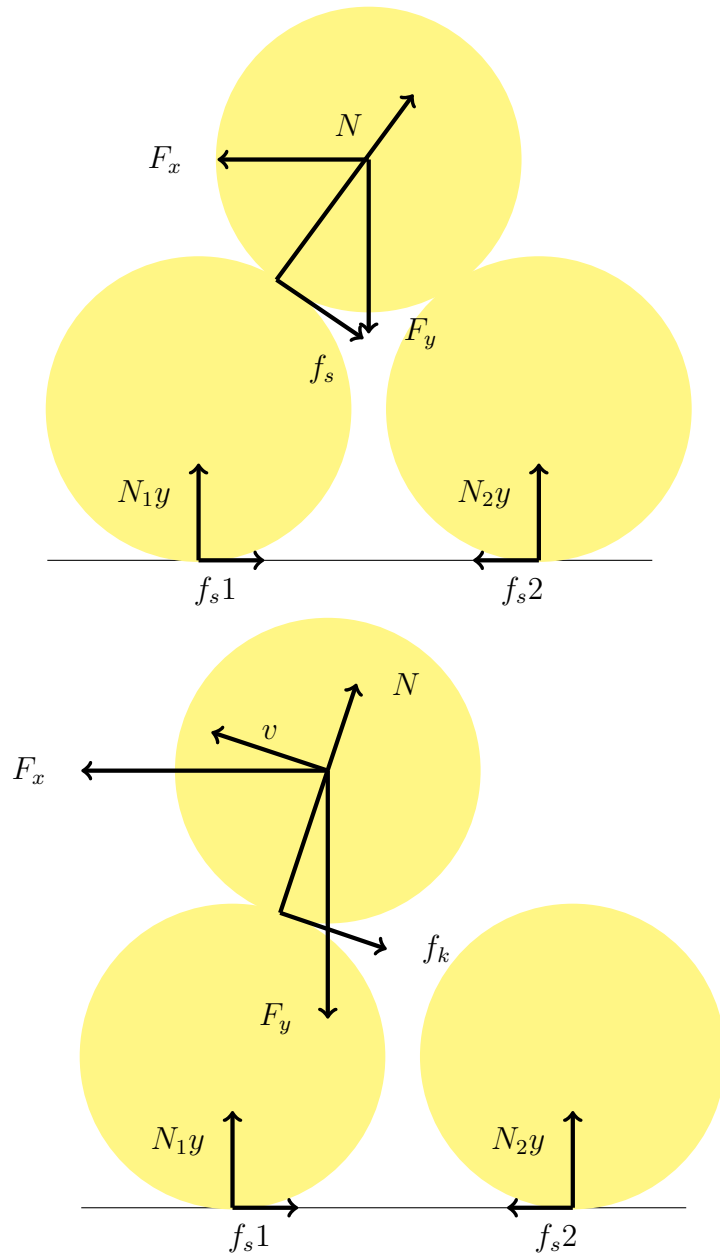


Figure 5.24: Simplified force scenario out of a wedge in a helical layout

Potential first layer complication

In the previous sections only the forces in between the two layers have been discussed, but these forces have implications that could lead to problems in the drum-tether contact surface. From both Figure 5.23 and Figure 5.24, it is clear that there are forces working between the drum-tether contact surface, namely N_1x , N_1y , f_2s and f_1s . The forces f_2s and f_1s are static frictional forces, and are the only ones keeping the first layer of the tether horizontally in place. This is visualized in a simplified figure in Figure 5.25. In this simplified scenario F is a combination of the F_x and F_y from Figure 5.24. This force will push on the first layer with different values upon contact (F_1 and F_2 in Figure 5.25). This will lead to respectively f_1s or f_2s needing to increase to resist horizontal motion. Previously it has been explained that the vigorous behavior of the tether when getting unwedged poses problems with extra pinching and crushing of the two layers, but it also poses a problem when considering the forces in the tether-drum contact surface. In the scenario when the tether goes over a wrap and hits the next wrap. The impact force would lead to either F_1 's or F_2 's x-component (depending on the spool direction) increasing notably. For a given normal force there are a maximum potential static friction force that could be present, and this maximum potential therefore has to withstand the force F from the vigorous overlap from one wedge to another, and depending on the size of F , that may not be possible. This would lead to the pitch between two wraps being extra large, while the pitch between the next two wraps would be smaller, which would lead to very uncontrolled spooling and potentially even greater pinching and crushing of the tether. Figure 5.25 clearly illustrates how the Lebus Layout removes this problem, as the normal force from the grooves are tilted, providing extra support for the tether to stay in place.

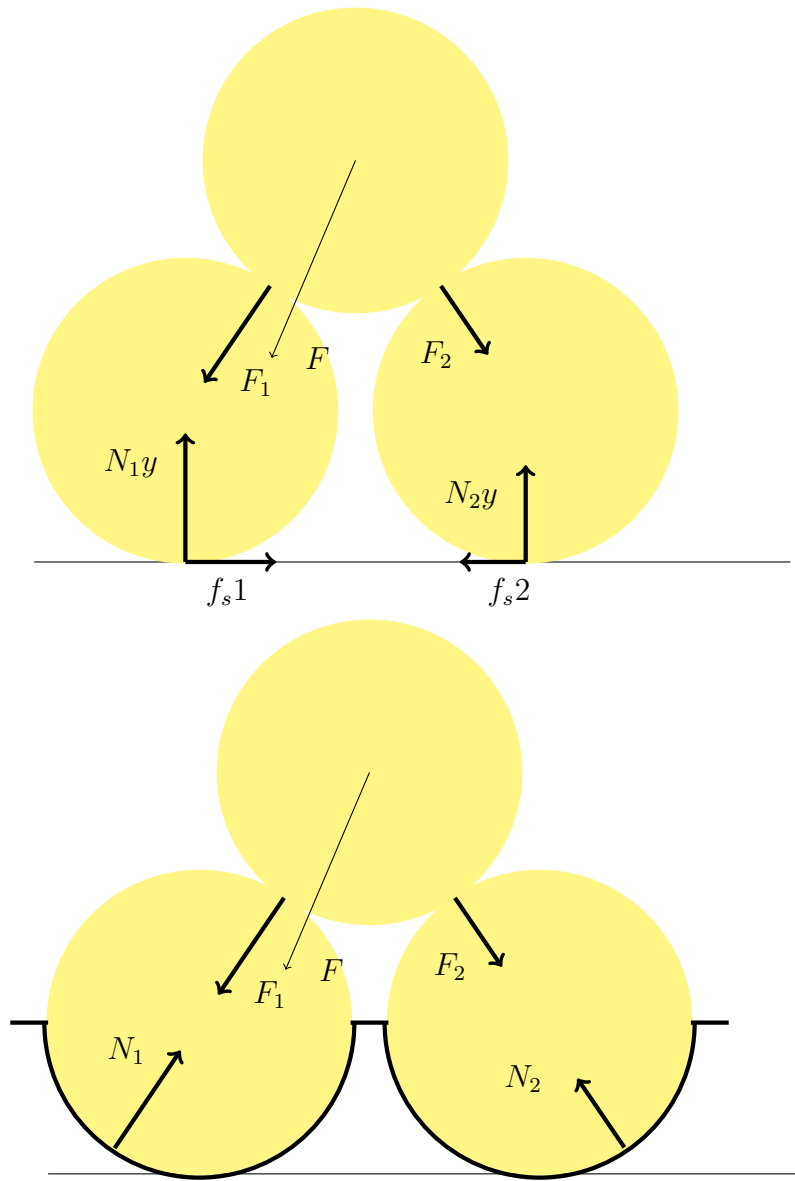


Figure 5.25: Smooth versus Lebus layout

Pitch considerations

From the discussion above it may seem like the best solution is to make the pitch as small as possible. First of all this would lead to a more compact solution with more cable in each layer. This would also lead to less wedging, and the wedging that would occur would lead to a smaller horizontal net force on the way out of the wedge, as the normal force would be tilted more vertically than with a larger wedge. The movement over a wrap would occur earlier, and in a less powerful manner. This would lead to less forces in the horizontal direction, both from N and F_x , meaning that the static frictional forces between the drum-tether surface would not be required to have such a large maximum potential force that it would need to deliver.

The tether has a outer diameter equal to 37.4mm. This is then the smallest pitch possible for the drum configuration. The groove made up from two wraps laying side by side would then be as small as possible, and wedging would not occur to the same extent as with an air gap in between them. This solution seems to be the best one, but that idea ignores the fact that the tether diameter has an uncertainty of $\pm 1\text{mm}$. In the first layer, when stacking the tethers side by side with no air gap, one would therefore get some places with some air gap. The foundation made up of the first layer will also be sloped, as the height of the tether will vary, and therefore further randomizing tether behavior. The uncertainty in tether diameter also poses a problem in the layout, namely how do one construct the end fillers if it is not certain how the tether is placed in the last wrap before contacting it. The uncertainty in the tether diameter means that there is no real way to determine the tether behavior when meeting the end filler. For example, say that the tether is wrapped around the drum with 30 wraps in each layer. Without calibrating the fleet angle compensator for this uncertainty, there would then be an uncertainty of $\pm 30\text{mm}$ for where the 30th wrap would get placed on the end filler. What is further complicating the matter is when arriving at the second layer. Say that one would be able to place the tether in the first layer such that the tether hits the end filler in the right place, one would then have the same problem in the second layer. This second layer would need to hit the right place on opposite end filler, but in this layer it gets even more complicated. In addition to the uncertainty in tether diameter, the wedging of the tether further complicates the process, to a point where it is not possible to predict the tether behavior.

Chapter 6

Conclusions

6.1 Material choice

In conclusion, it is not possible to determine a specific rubber compound for the tension wheel of the TMS. However, it is believed that a compound made out of a nitrile base with some amount of different additives is the best option. Different nitrile compounds should be further investigated, with respect to the preference of attributes as compression set, creep, abrasion resistance and the other factors mentioned in the analysis, but one should prioritize friction over wear. The consequence of prioritizing wear, could lead to a material with excellent wear properties but lacking frictional properties, resulting in the TMS not working properly.

Future student/engineers working on this problem should explore rubber compounds and how different additives affect their characteristics more carefully, preferably with testing of the materials in similar environment as the TMS. Another idea is to study what the implementation of treads, like in car tire, does to the wear and frictional properties of the tension wheel.

6.2 Choosing a friction model

In the analysis part of the thesis, the necessary friction coefficients was calculated for the different friction models. For the no squeeze models using the U- and V-shaped tension wheel, one of the assumptions necessary to do calculations with the capstan equation was that the outboard part of the tether was in a given amount of tension relative to the inboard part of the tether. This value was set to one tenth of the inboard tether tension. As this might be true during many stages of operation, it is not necessarily constant

nor as large as assumed at any given point. As the friction coefficient found is highly dependent on the ratio between the outboard and inboard tension, a smaller value of outboard tension drastically changes the friction coefficient necessary.

For this reason, the conclusion is that one is best served using some squeezing to operate the TMS properly, as the outboard tension does not to any measurable extent affect how large of a friction coefficient is needed. To optimize squeezing it is proposed that compression testing of the TPR rubber material is conducted. This will easily give IKM the knowledge of how much squeeze the tether can be exposed to, without there being any danger of z-kinks and still be able to operate the TMS in a controlled fashion. One could also go about changing the tether used, to a tether with a thicker outer rubber sheet, in order to create a larger safe-squeeze interval.

6.3 Rewinding algorithm improvement

As stated in section 5.4, to make a winding algorithm without the use of a Lebus Shell, a helical layout would need to be applied. Due to the reasoning made in the same section, the application of this solution is not as easy as one would first think. There are many extra factors that need to be taken into consideration when altering the layout from Lebus to helical. These factors are in addition spontaneous, making them very hard to predict. For such a solution to be applied, the spooling would need to be adjusted in regards to the uncertainties in the tether supplied. One would need to observe the tether behavior when adjusting the fleet angle and spool speed, and see how this impacts the pitch, and again how this affects the violent wrapping behavior. When getting a pitch that makes the tether hit the first end filler in a desired manner, one would go onto the next layer and try and fail until finding a fleet angle and spool speed that makes the tether hit the second end filler correctly. This would need to be done in regards to all the possible complications discussed in section 5.4. One of the flaws of such a try and fail approach, is that in the event of a tether replacement, even when replacing it with an identical tether, the configuration would most likely need to be done all over again to account for the uncertainty in tether diameter. All in all an alteration to a helical layout would lead to the need for extensive testing and research, which would need to be weighed up against the economical cost of applying a Lebus shell layout to the drum.

Bibliography

- [1] Richard J. Schmidt Arthur P. Boresi. *Advanced Mechanics of Materials, sixth edition*. Wiley, 2003. ISBN: 978-0-471-43881-6.
- [2] Ali Asadi and Mike Brown. “Rail vehicle wheel wear prediction: a comparison between analytical and experimental approaches”. In: *Vehicle System Dynamics* 46.6 (2008), pp. 541–549. DOI: 10.1080/00423110701589430. eprint: <https://doi.org/10.1080/00423110701589430>. URL: <https://doi.org/10.1080/00423110701589430>.
- [3] AZoM. *Properties, an introduction to copper*. URL: <https://www.azom.com/properties.aspx?ArticleID=597> (visited on 12/05/2021).
- [4] Prestice BDT. *PRACTICAL TYRE MODELS: SLIP ANGLE AND SLIP RATIO*. U.D. URL: <https://www.presticebd.com/slip-angle-and-slip-ratio-definition/>.
- [5] Peter J Blau. “The significance and use of the friction coefficient”. In: *Tribology International* 34.9 (2001), pp. 585–591. ISSN: 0301-679X. DOI: [https://doi.org/10.1016/S0301-679X\(01\)00050-0](https://doi.org/10.1016/S0301-679X(01)00050-0). URL: <https://www.sciencedirect.com/science/article/pii/S0301679X01000500>.
- [6] Robert W Bruce. *Handbook of lubrication and tribology, volume ii : Theory and design, second edition*. Taylor Francis Group, 2012. ISBN: 9781420069099.
- [7] Wes Cash. *Lubrication Meaning*. URL: <https://www.machinerylubrication.com/Read/28766/what-is-lubrication>.
- [8] Allan G. Piersol Cyril M. Harris. *Harris’ Shock and Vibration Handbook*. McGraw-Hill, 2002. ISBN: 0071370811.
- [9] Inc. Datwyler Sealing Solutions USA. *Rubber Materials Elastomer Compound Information*. U.D. URL: <http://usa.datwyler.com/materials.html>.
- [10] Jiri George Drobny. *Handbook of Thermoplastic Elastomers*. Elsevier Science Technology Books, 2014. ISBN: 9780323221689.

- [11] “25 - Friction and wear”. In: *Smithells Metals Reference Book (Eighth Edition)*. Ed. by W.F. Gale and T.C. Totemeier. Eighth Edition. Oxford: Butterworth-Heinemann, 2004, pp. 25-1-25–26. ISBN: 978-0-7506-7509-3. DOI: <https://doi.org/10.1016/B978-075067509-3/50028-2>. URL: <https://www.sciencedirect.com/science/article/pii/B9780750675093500282>.
- [12] Lebus Germany. *The original parallel groove spooling system*. U.D. 2009. URL: <https://lebus-germany.com/Downloads/dl-lebus-brochure-2009.pdf>.
- [13] Erik Gregersen. *Coefficient of friction*. URL: <https://www.britannica.com/science/coefficient-of-friction> (visited on 08/02/2021).
- [14] Øyvind Grøn. *friksjon*. Nov. 2020. URL: <https://snl.no/friksjon> (visited on 08/02/2021).
- [15] Dorian A.H. Hanaor, Yixiang Gan, and Itai Einav. “Static friction at fractal interfaces”. In: *Tribology International* 93 (2016), pp. 229–238. ISSN: 0301-679X. DOI: <https://doi.org/10.1016/j.triboint.2015.09.016>. URL: <https://www.sciencedirect.com/science/article/pii/S0301679X15004181>.
- [16] Xinwu Huang et al. “Friction and wear properties of NBR/PVC composites”. In: *Journal of Applied Polymer Science* 106.4 (2007), pp. 2565–2570. DOI: <https://doi.org/10.1002/app.25316>. eprint: <https://onlinelibrary.wiley.com/doi/pdf/10.1002/app.25316>. URL: <https://onlinelibrary.wiley.com/doi/abs/10.1002/app.25316>.
- [17] Hultec. *TYPICAL PROPERTIES OF ELASTOMERS*. U.D. URL: <http://www.hultec.com/wp-content/uploads/2014/05/Rubber-Properties-Chart.pdf>.
- [18] Jean Lemaitre Jean LeMaitre. *Handbook of Materials Behavior Models, Three-Volume Set*. Elsevier Science Technology, 2011. ISBN: 9780080533636.
- [19] Daniel L. Hertz Jr. “An analysis of rubber under strain from an engineering perspective”. In: *Elastomerics* (1991). URL: <https://www.sealseastern.com/PDF/RubberUnderStrain.pdf>.
- [20] Joshua Leimkuehler. *Chevrolet Silverado: Brake Diagnostics Guide*. July 2015. URL: <https://chevroletforum.com/how-tos/a/chevrolet-silverado-brake-diagnostics-guide-389668>.
- [21] Laurence W. McKeen. *The Effect of Creep and Other Time Related Factors on Plastics and Elastomers*. Elsevier Science Technology Books, 2002014. ISBN: 9780323354073.

- [22] Ranganathan Mohan, B. Das, and Raja Sundaresan. “Effect of Hardness and Surface Roughness on Slip Resistance of Rubber”. In: *Journal of Testing and Evaluation* 43 (Nov. 2015), p. 20140249. DOI: 10.1520/JTE20140249.
- [23] A. Mostafa et al. “Effect of carbon black loading on the swelling and compression set behavior of SBR and NBR rubber compounds”. In: *Materials Design* 30.5 (2009), pp. 1561–1568. ISSN: 0261-3069. DOI: <https://doi.org/10.1016/j.matdes.2008.07.043>. URL: <https://www.sciencedirect.com/science/article/pii/S0261306908003865>.
- [24] Nagaraj S. Nayak P.A. Lakshminarayanan. *Critical component wear in heavy duty engines*. John Wiley Sons, Incorporated, 2011. ISBN: 9780470828830.
- [25] Valentin L. Popov. *Contact Mechanics and Friction*. Springer-Verlag Berlin Heidelberg, 2010. ISBN: 9783642108020.
- [26] White Cross Rubber Products. *Which Elastomer Offers The Best Abrasion Resistance?* U.D. URL: <https://wcrp.uk.com/technical/material-selection/which-elastomer-offers-the-best-abrasion-resistance/>.
- [27] Material Properties. *What is Surface Fatigue – Fatigue Wear – Definition*. URL: <https://material-properties.org/what-is-surface-fatigue-fatigue-wear-definition/> (visited on 12/04/2021).
- [28] J.K. Gupta R.S. Khurmi. *A textbook of machine design*. Eurasia Publishing House (PVT.) LTD., 2005.
- [29] Paulo Cachim Rafat Siddique. *Waste and Supplementary Cementitious Materials in Concrete*. Elsevier Science Technology, 2018. ISBN: 9780081021576.
- [30] Jr. Raymond A. Serway John W. Jewett. *FYS100 Fysikk*. Cengage Learning EMEA, 2017. ISBN: 9781473754898.
- [31] Rivania Rezende et al. “NUMERICAL MODELING OF ELASTOMERIC SUPPORT DEVICES IN BRIDGE BEAMS”. In: Nov. 2019.
- [32] Rivania Rezende et al. “NUMERICAL MODELING OF ELASTOMERIC SUPPORT DEVICES IN BRIDGE BEAMS”. In: Nov. 2019.
- [33] J-Flex Innovative rubber solutions. *How is Rubber Hardness measured? What does Shore Hardness mean?* U.D. URL: <https://www.j-flex.com/how-is-rubber-hardness-measured-what-does-shore-hardness-mean/>.

- [34] Cameron Tracy et al. *Cohesive and Adhesive Forces*. Aug. 2020. URL: [https://chem.libretexts.org/Bookshelves/Physical_and_Theoretical_Chemistry_Textbook_Maps/Supplemental_Modules_\(Physical_and_Theoretical_Chemistry\)/Physical_Properties_of_Matter/States_of_Matter/Properties_of_Liquids/Cohesive_and_Adhesive_Forces](https://chem.libretexts.org/Bookshelves/Physical_and_Theoretical_Chemistry_Textbook_Maps/Supplemental_Modules_(Physical_and_Theoretical_Chemistry)/Physical_Properties_of_Matter/States_of_Matter/Properties_of_Liquids/Cohesive_and_Adhesive_Forces).
- [35] Leslie R.G. Treloar. *The Physics of Rubber Elasticity*. Oxford, 1975. ISBN: 978-0-198-51355-1.
- [36] Team Tyremarket.com. *What Is A Tread Wear Indicator?* U.D. U.D. URL: <https://www.tyremarket.com/tyremantra/tread-wear-indicator/>.
- [37] U.D. *Capstan equation*. URL: https://en.wikipedia.org/wiki/Capstan_equation (visited on 06/04/2021).
- [38] Roland Verreet. *New wire rope designs for multi layer drums*. 2019. URL: http://www.ropetechnology.com/bro_engl/Bro_Mehrlagen_en.pdf (visited on 06/04/2021).
- [39] E.A.H. Vollebregt and H.M. Schuttelaars. “Quasi-static analysis of two-dimensional rolling contact with slip-velocity dependent friction”. In: *Journal of Sound and Vibration* 331.9 (2012), pp. 2141–2155. ISSN: 0022-460X. DOI: <https://doi.org/10.1016/j.jsv.2012.01.011>. URL: <https://www.sciencedirect.com/science/article/pii/S0022460X12000314>.
- [40] John A. Williams. “Wear and wear particles—some fundamentals”. In: *Tribology International* 38.10 (2005). Ferrography and Friends - Pioneering Developments in Wear Debris Analysis, pp. 863–870. ISSN: 0301-679X. DOI: <https://doi.org/10.1016/j.triboint.2005.03.007>. URL: <https://www.sciencedirect.com/science/article/pii/S0301679X05000903>.